bioRxiv preprint doi: https://doi.org/10.1101/106591; this version posted February 16, 2017. The copyright holder for this preprint (which was not certified by peer review) is the author/funder. All rights reserved. No reuse allowed without permission.

Small molecule–mediated reprogramming of the epithelial–mesenchymal transition prevents fibrosis

Running title: Reversion of fibrosis by chromones

Han-Soo Kim,[1,2*] Jun-Hwan Kim,[1,3*] Ji Yong Lee,[2] Young-Min Yoon,[3] Ik-Hwan Kim,[4] Ho-Sup Yoon[5] and Byung-Soo Youn[3#]

[1]Institute for BioMedical Convergence, Catholic Kwandong University-International St. Mary's Hospital, Incheon 22711, Republic of Korea , [2]Department of Biomedical Sciences, Catholic Kwandong University College of Medicine, Gangneung-si, Gangwon-do 25601, Republic of Korea. [3]#705 Ace High-end Tower 9th 233,Gasandigital-1-ro, Geumcheon-gu, Seoul, 08501, Republic of Korea, [4]Department of Biotechnology, Korea University. Seoul 02841and [5]Department of Genetic Engineering, College of Life Sciences, Kyung Hee University, Yongin-si, Gyeonggi-do 446-701, Republic of Korea and [5]School of Biological Sciences, Nanyang Technological University, 60 Nanyang Drive, 637551, Singapore

*These contributes equally to this work.

[#]**Corresponding author**:

Byung-Soo Youn, PhD, OsteoNeuroGen, Inc. Ace High-end Tower 9th 233, Gasandigital-1-ro, Geumcheon-gu, Seoul, 08501, Republic of Korea

Email: byung4jc@gmail.com, Tel) 822- 6267 2737 Fax) 822-6267-2740

bioRxiv preprint doi: https://doi.org/10.1101/106591; this version posted February 16, 2017. The copyright holder for this preprint (which was not certified by peer review) is the author/funder. All rights reserved. No reuse allowed without permission.

Abstract

Fibrosis is an intractable human disease for which no curative drugs have yet been developed. Recent work revealed that renal fibrosis is a manifestation of the epithelial–mesenchymal transition (EMT). Chromones and chromone derivatives (CDs) are compounds based on a chemical scaffold found ubiquitously throughout the plant kingdom. We recently showed that eupatilin, a CD from an *Artemisia* species, efficiently shuts down osteoclastogenesis, concomitant with global downregulation of EMT-associated genes. For this study, we established the mouse hepatic stellate cell (HSC) line ONGHEPA1.Real-time imaging revealed that upon stimulation with TGFβ, ONGHEPA1 cells uniformly differentiated into myofibroblasts, but fibrosis was completely inhibited by 50 μM eupatilin. Concomitant with these anti-fibrotic effects, multiple EMT-inducible genes, such as *Col11a1*, *periostin* and *Slit3,* were significantly downregulated. Although pretreatment with eupatilin did not affect the anti-fibrotic effect by TGFβ, stimulation with eupatilin following pretreatment with TGFβ completely blocked fibrosis, suggesting that the anti-fibrotic capacity of eupatilin is tightly coupled to TGFβ signaling components or TGFβ-inducible molecules. This observation led us to hypothesize that eupatilin could reverse fibrosis in ONGHEPA1 cells by reprogramming the EMT. When ONGHEPA1 cells were sequentially stimulated and differentiated into fibroblasts with TGFβ and eupatilin or selected CDs, we observed dramatic morphological changes along with reversal of the EMT. RNA-Seq analyses and interactome studies revealed that multiple genes involved in the EMT were induced by TGFβ, but repressed by eupatilin. We identified 103 genes whose expression reached the highest levels following stimulation with TGFβ, but dropped to basal levels in cells treated with eupatilin. The majority of these genes were EMT-associated. A defined set of 34 CDs was tested in the fibrosis assay, leading to the

bioRxiv preprint doi: https://doi.org/10.1101/106591; this version posted February 16, 2017. The copyright holder for this preprint (which was not certified by peer review) is the author/funder. All rights reserved. No reuse allowed without permission.

identification of two additional CDs capable of blocking the EMT as effectively as eupatilin. The methoxy residue at the sixth carbon (C6) on the chromone scaffold is essential for anti-fibrotic effects, and the hydroxy residue at C7 is also important. However, the presence of any functional groups at C2 significantly decreased anti-fibrotic activity. Replacement of the chemical residues of the remaining carbons (C1, C3, and C4) with methoxy groups led to toxicity or apoptosis. To evaluate the suitability of eupatilin for treating human idiopathic pulmonary fibrosis (IPF), we used a mouse model of bleomycin-induced lung fibrosis. From a histopathological perspective, eupatilin significantly decreased disease severity, reducing infiltration of lymphocytes as well as the extent of extracellular matrix deposits. Taken together, our findings reveal a novel and potent EMT-inhibitory activity associated with the chromone scaffold, which is capable of reversing fulminant fibrosis to the normal state.

bioRxiv preprint doi: https://doi.org/10.1101/106591; this version posted February 16, 2017. The copyright holder for this preprint (which was not certified by peer review) is the author/funder. All rights reserved. No reuse allowed without permission.

Introduction

Fibrosis is a complex disease state in which elevated proliferation of myofibroblasts is accompanied by overproduction of extracellular matrix (ECM) components, resulting in cellular stiffness (Bonnans et al. 2014). The cellular players in this process are diverse, and the identities of key cell types depend on tissue context (Murray 2016). Idiopathic pulmonary fibrosis (IPF) and liver fibrosis affect many people around the world, representing an urgent medical need. To date, however, no curative drugs have become available to treat these conditions (Fallowfield 2015, Sgalla et al. 2016). Two small-molecule anti-fibrotic drugs, pirfenidone (Esbriet) and nintedanib (Ofev), have been recently adopted for IPF (King and Nathan 2015), but their efficacies and side effects must be improved to successfully treat this disease. Moreover, the underlying molecular and cellular mechanisms through which these drugs exert their anti-fibrotic activities against IPF need to be more completely elucidated. Although liver fibrosis afflicts more people than IPF around the world (Poynard et al. 2010), no drugs are currently available to treat this disorder.

Liver fibrosis is an inflammatory disease elicited by type 2 immunity, and is associated with massive proliferation of fibroblasts and differentiation of stem cell–like hepatic stellate cells (HSCs) into myofibroblasts (Yin et al 2013). Recent work showed that renal fibrosis is mediated by EMT, a well-defined cellular program that plays a major role in promoting tumor metastasis (Lamouille et al. 2014). A set of *Twist* or *Snail*-regulating genes contributes to renal fibrosis and other types of fibrotic disorders (Lovisa et al. 2015), suggesting that downstream genes of *Twist* or *Snail*, such as collagens and adhesion molecules, promote fibrosis. Hence, the EMT has been recognized as a central program driving diverse cellular dysfunctions, and

bioRxiv preprint doi: https://doi.org/10.1101/106591; this version posted February 16, 2017. The copyright holder for this preprint (which was not certified by peer review) is the author/funder. All rights reserved. No reuse allowed without permission.

thus represents a promising molecular therapeutic target for many intractable human diseases that decrease the quality of life, including fibrotic disorders.

Flavones or isoflavones are members of the polyphenol family, a group of >10,000 compounds that are predominantly found in the plant kingdom (Dixon and Pasinetti 2010). Among other functions, these phytochemicals protect plants from radiation damage (Stapleton and Walbot 1994). Due to their anti-oxidant and anti-inflammatory potential, flavones have long been used to treat inflammatory diseases such as arthritis or asthma (Leyva-López et al. 2016). Chromone (1,4-benzopyrone-4-one) is a chemical scaffold present in a large number of flavones (Emami and Ghanbarimasir 2015), and the chromone derivatives (CDs) are a diverse family based on this core chemical framework (Gacche et al. 2015). We recently reported that eupatilin, a CD from an *Artemisia* species, dramatically inhibited osteoclastogenesis (Kim et al. 2015) and downregulated multiple genes associated with the EMT, as revealed by RNA-Seq analysis (*Supplementary figure. 1A*). This observation prompted us to hypothesize that eupatilin might prevent fibrosis.

Here, we show that selected CDs can reprogram EMT, thereby ameliorating fibrosis. Because these new compounds could be used in combination with existing drugs for IPF, potentially achieving synergistic effects, the observation opens the door to a powerful new therapeutic modality for treating generalized fibrosis.

bioRxiv preprint doi: https://doi.org/10.1101/106591; this version posted February 16, 2017. The copyright holder for this preprint (which was not certified by peer review) is the author/funder. All rights reserved. No reuse allowed without permission.

Results & Discussion

CDs inhibit fibrosis by reversing changes in cell morphology

To test this hypothesis, we established the HSC line ONGHEPA1 as an *in vitro* model of mouse liver fibrosis. HSCs are widely appreciated for their roles in initiation and perpetuation of liver fibrosis (Gabele et al. 2003). ONGHEPA1 cells, which have a mesenchymal morphology (*Supplementary figure. 1B*), expressed GATA4 but not cytokeratin 18 (*Supplementary figure. 1C*), strongly indicating that they have an endodermal origin and are not related to epithelial cells. No albumin was detected (data not shown).

When ONGHEPA1 cells were stimulated with TGFβ, significant morphological changes occurred 6–8 h after stimulation, and full commitment to myofibroblasts occurred by 24–48 h (*Supplementary figure 2*). Eupatilin, produced in a seven-step synthesis and purified to homogeneity at GLP levels (*Supplementary figure 3*), completely inhibited TGFβ-induced fibrosis at a concentration of 50 μM (Figure 1A). Immunocellularchemistry (ICC) experiments clearly demonstrated that immune-reactivity to α smooth muscle actin after TGFβ stimulation was significantly decreased by eupatlin. PDGF also contributes to fibrosis (Andrae et al. 2008). As shown in *Supplementary figure 4, ONGHEPA*1 exhibited an earlier response to PDGF than TGFβ, but the resultant pattern of fibrosis was not significantly different. Eupatilin also completely inhibited PDGF-induced fibrosis as well as immune-reactivity to α smooth muscle actin (Figure 1B).

To avoid potentially confounding effects of serum on differentiation, differentiation of HSC into fibroblasts by TGFβ treatment was conducted in serum-free medium in which proliferation was inhibited, confirming the anti-fibrotic effect of eupatilin (Figure 1C).

bioRxiv preprint doi: https://doi.org/10.1101/106591; this version posted February 16, 2017. The copyright holder for this preprint (which was not certified by peer review) is the author/funder. All rights reserved. No reuse allowed without permission.

Finally, we investigated whether fibrosis induced by TGFβ or PDGF could be inhibited by CDs including eupatilin in normal human lung fibroblasts (NHLFs), major cellular players associated with IPF (Huang et al. 2014). Since responsiveness of NHLFs to TGFβ stimulation is a little different from that of the fibroblasts differentiated from ONGHEPA1 cells PDGF-mediated fibrosis in NHLF cells is to be mainly described. Eupatilin and two CDs called ONGE200 and ONGA300 markedly prevented fibrosis induced by PDGF in these cells (Figure 2A). CD-treated NHLFs exhibited retarded growth rate and gross change in morphology. ONGE200 seemed to be a little toxic, which is contrasted to the anti-fibrotic effect of ONGE200 on ONGHEPA1 cells. The similar cytotoxicity was seen from stimulation of NHLFs with TGFβ (*Supplementary figure 5A*). Immnuocellularchemistry (ICC) experiments demonstrated that the immune-reactivity to α smooth muscle actin after PDGF stimulation was significantly diminished by eupatlin (Figure 2B). Real-time PCR showed that *coll11α1*, *vimenin*, or *periostin* expression was decreased by eupatilin, suggesting the EMT is significantly inhibited by eupatilin (Figure 2C). The immunoreactivity to α smooth muscle actin in the NHLFs stimulated by TGFβ was increased and markedly deceased by eupatilin (*Supplementary figure 5B*). However, we consistently observed that the gene expression of *col11α1* and *vimentin* was upregulated by eupatilin but *periostin* was far downregulated (*Supplementary figure 5C*), suggesting that regulation of EMT components by small molecules might be diverse or would rather be flexible depending cellular contexts. Real-time imaging experiments conducted for 24 h confirmed that TGFβ significantly induced fibrosis whereas eupatilin completely inhibited it (*Supplementary figure 6*).

bioRxiv preprint doi: https://doi.org/10.1101/106591; this version posted February 16, 2017. The copyright holder for this preprint (which was not certified by peer review) is the author/funder. All rights reserved. No reuse allowed without permission.

Specific carbons of the chromone scaffold and chemical residues are critical for anti-fibrotic effects

Next, we selected 34 CDs with chemical similarity to eupatilin and evaluated their anti-fibrotic effects (*Supplementary figure 7*). We identified three CDs as active: eupatilin itself, ONGE200 (also known as hispidulin), and ONGA300 (also known as jaceosidin). The latter two compounds were the most closely chemically related to eupatilin among CDs tested. Chemical differences are highlighted in Figure 3. The eight conserved CD carbons are represented in colored letters, whereas differences in the phenyl residues connected to the chromone scaffold are indicated by blue boxes. In rats, ONGA300 has been identified as a plasma metabolite generated by decarboxylation of eupatilin, and was also detected along with eupatilin in an *Artemisia* extract (Ji et al. 2010). The anti-fibrotic effects of eupatilin and ONGE200 were concentration dependent (Figure 3A and Figure 3B); ONGA300 was cytotoxic at 50 μM, but exerted clear anti-fibrotic effects at a much lower concentration, 10 μM (Figure 3C). To explore the importance of the eight carbons of the chromone scaffold in terms of structure–function relationship, we compared the three active CDs with the other compounds in the test set. When the dimethoxy residues of eupatilin were replaced with dihydroxy groups, as seen in ONGI300, the anti-fibrotic effect was eliminated (Figure 3D4D). However, hemi-replacement of the dimethoxy residues with a hydroxy group, as in ONGA300 (jaceosidin), preserved the anti-fibrotic effect at 10 μM. Together, these observations suggest that the functional residues of the phenyl group bonded to the chromone scaffold play important roles in inhibiting fibrosis.

We further characterized the importance of the eight carbons by profiling CDs. In comparison with ONGE200, ONGI200 (also known as apigenin) lacks only the methoxy group

bioRxiv preprint doi: https://doi.org/10.1101/106591; this version posted February 16, 2017. The copyright holder for this preprint (which was not certified by peer review) is the author/funder. All rights reserved. No reuse allowed without permission.

bonded to the C6th carbon (C6). However, ONGI200 exerted no anti-fibrotic effects, suggesting that C6 is an important constituent of the chromone scaffold, and that attachment of a methoxy residue to C6 is necessary for prevention of fibrosis (Figure 3E). We also noticed that ONGC200, in which the hydroxy residue of ONGE200 is replaced with a methoxy group, completely lost the anti-fibrotic effect, suggesting the C7 is also a critical component of chromone scaffold (denoted by a blue circle in *Supplementary figure 8-1*). In addition, methoxylation of C2 of ONGA300, generating a compound equivalent to ONGH300, abolished anti-fibrotic capacity, suggesting that the presence of a bulky group at C2 affects anti-fibrotic potential (Figure 3F). The same held true for ONGD400, a highly cytotoxic stereoisomer of ONGH300, as denoted by the blue arrow and figure in *Supplementary figure 8-2.* Taken together, our data confirm that substitutions on the chromone scaffold were only tolerated in specific cases, indicating a stringent structure–activity relationship (SAR) in regard to chromones' anti-fibrotic effects (Figure 4).

The anti-fibrotic capacity of selected CDs requires stimulation with TGFβ and is mediated by reprogramming EMT

To determine whether receptor(s) or a binding protein(s) for the CDs identified in the previous section exist, and if so, whether these factors mediate the anti-fibrotic effect, we pretreated ONGHEPA1 with eupatilin at various time points for up to 6 hr, the time at which pretreatment of BMM with eupatilin completely blocks osteoclastogenesis (Kim, et al. 2015). Figure 5A shows that, compared with control treatments, eupatilin had clear anti-fibrotic activity. In contrast to the effect on osteoclastogenesis, pretreatment of ONGHEPA1 cells with eupatilin did not prevent fibrosis (Figure 5B); however, pretreatment of ONGHEPA1 cells

bioRxiv preprint doi: https://doi.org/10.1101/106591; this version posted February 16, 2017. The copyright holder for this preprint (which was not certified by peer review) is the author/funder. All rights reserved. No reuse allowed without permission.

with TGFβ followed by eupatilin treatment completely inhibited fibrosis, suggesting that the effect of eupatilin depends on TGFβ pathway components or TGFβ-inducible proteins (Figure 5C).

We previously observed that fibrogenesis in ONGHEPA1 cells occurred 6 hr after TGFβ stimulation (*Supplementary figure 2*). Therefore, we hypothesized that the selected CDs could reverse preexisting fibrosis. To test this hypotheses, we treated ONGHEPA1 cells sequentially with TGFβ for 24 hr, leading to 100% conversion into fibroblasts; washed them with PBS, and then finally re-stimulated with TGFβ or PDGF plus selected CDs for 24 hr. Under these conditions, fibroblasts were converted into ONGHEPA1-like cells, as shown in Figure 6A and 6B. This morphological reversion was highly correlated with downregulation of certain EMT-related genes, including *Col11a1* (collagen 11a1), *Slit3* (Slit homolog 3), *Axl* (receptor tyrosine kinase), *Postn* (periostin), *Fn1* (fibronectin 1), and *Aurka* (Aurora kinase). *Axl* (a receptor kinase) expression differed in response to TGFβ and PDGF (Figure 6C and 6D), but the reason for this difference remains unknown. We extensively confirmed the anti-fibrotic capacities of eupatilin, ONGE200, and ONGA300 in simultaneous or sequential stimulation conditions, as shown in Figure 7A, 7B, and 7C, respectively. The data clearly demonstrated that these selected CDs were capable of preventing the establishment of fibrosis, as well as reversing fibrosis that already existed. Sequential stimulation experiments with TGFβ or PDGF were also conducted using the remaining 31 CDs in the test set (*Supplementary figures 9-1, 9-2, 10-1 and 10-2*). None of these compounds exhibited reversion activity, and some were cytotoxic, again confirming that eupatilin, ONGE200, and ONGA300 were the only CD members capable of reversing fibrosis. Finally, real-time imaging revealed the morphological reversal of fibroblasts into ONGHEPA1-like cells (*Supplementary figure 11*).

bioRxiv preprint doi: https://doi.org/10.1101/106591; this version posted February 16, 2017. The copyright holder for this preprint (which was not certified by peer review) is the author/funder. All rights reserved. No reuse allowed without permission.

Reprogramming EMT by the selected CD members is responsible for anti-fibrosis

We next asked whether eupatilin could inhibit EMT induced by TGFβ with simultaneous stimulation or committed EMT via sequential stimulation. To demonstrate the former, we stimulated ONGHEPA1 cells with TGFβ or TGFβ plus eupatilin, and then conducted global gene expression analyses using RNA-Seq. A 60 Gb sequence was generated, which showed clear Volcano plots as shown in *Supplementary figure 12A*. A total of 10,020 transcripts were read and compared. When ONGHEPA1 cells were stimulated with TGFβ, 826 genes were induced. Treatment of TGFβ-treated ONGHEPA1 cells with eupatilin specifically induced 150 genes, (*Supplementary figure 12B)*. While the identity of the genes with altered expression between TGFβ-treated ONGHEPA1 cells and TGFβ plus eupatilin-treated ONGHEPA1 cells via simultaneous stimulation (*Supplementary table 1)* was 85.4%. identity was 81.0% between TGFβ-treated ONGHEPA1 cells and ONGHEPA1 cells sequentially treated with a combination of TGFβ and eupatilin (*Supplementary table 2).* In the case of sequential stimulation, although the reversion to a normal ONGHEPA1-like morphology was evident, the identity of genes with altered expression between TGFβ-treated and TGFβ plus eupatilin–treated ONGHEPA1 cells was 81%. RNA-Seq analysis under the sequential stimulation condition was conducted by using highly confluent cells, which could have affected changes in gene expression induced by eupatilin. Gene Ontology analysis revealed that under both stimulation conditions, the genes with the largest changes in expression encoded proteins classified as cellular components (7% and 20.5%, respectively), suggesting that eupatilin's mode of action is related to its ability to induce morphological changes via its effects on cytoskeletal protein expression. Using bioinformatics, we constructed an unbiased interactome

bioRxiv preprint doi: https://doi.org/10.1101/106591; this version posted February 16, 2017. The copyright holder for this preprint (which was not certified by peer review) is the author/funder. All rights reserved. No reuse allowed without permission.

(Figure 8), revealing several notable hubs, including the collagen gene family (*Col11α1*) and the cytoskeletal gene family (*Actin* α *smooth muscle aorta, Troponin 1* and *2, Tropomyosin 2, Myosin-heavy chain 1* and *Myosin-light chain 9*, and *Laminin 4*). Notably, *integrin α1* and *integrin β3* played pivotal roles in connecting these two gene hubs. Expression of *Slug, Zeb1,* and *Gli1*, major transcription factors deeply involved in the EMT, was inhibited by eupatilin. Several receptor-encoding genes, such as the semaphorin receptor family, a cholesterol receptor (*Vldr*), and *CD44*, formed significant hubs one notable signaling molecule associated with eupatilin-mediated reprogramming EMT was adenylate cyclase 9 (*Adcy9*), which might be triggered by cell-associated small-molecule ligand(s), leading to small G-protein activation (*Supplementary table 3*). To identify the most critical genes involved in reprogramming EMT by eupatilin, we identified a gene set that was maximally induced by TGFβ and maximally repressed by eupatilin; the resultant set of 103 genes is listed in *Supplementary table 4*. The vast majority of these genes are involved in promoting the EMT. For an instance, follistatin-like 1 (*Fstl1*) plays a pivotal role in pulmonary fibrosis (Dong et al. 2015), and deficiency of *Fstl*1 completely protects mice from bleomycin-induced lung fibrosis, consistent with the downregulation of *Fstl1* by eupatilin. These eupatilin-repressible genes could be new molecular targets for fibrosis.

In summary, the data presented in this section indicate that selected CDs (eupatilin, ONGE200, and ONGA300) reprogram the EMT, curbing fibrosis in a cell culture model.

Eupatilin significantly improves bleomycin-induced lung fibrosis

Finally, to assess the ability of eupatilin to inhibit fibrosis *in vivo*, we used a mouse

bioRxiv preprint doi: https://doi.org/10.1101/106591; this version posted February 16, 2017. The copyright holder for this preprint (which was not certified by peer review) is the author/funder. All rights reserved. No reuse allowed without permission.

model of bleomycin-induced lung fibrosis. Each test group consisted of five 5-week-old male C57BL/6J mice, as summarized in *Supplementary table 5*. Three mice per test group were selected, and their lung tissues were excised. Pulmonary fibrosis was induced by intratracheal administration of bleomycin for 12 days, followed by administration of 1–40 μg of eupatilin via the nose. Pulmonary fibrosis was more effectively inhibited by 20 μg or 40 μg of eupatilin, and the animals receiving these doses exhibited significant clearance of ECM, as revealed by Masson's trichrome staining (Figure 9A). Concomitant with inhibition of lung fibrosis by eupatilin, infiltration of lymphocytes was significantly inhibited, but monocytes were not affected (Figure 9B*)*, consistent with the observation that type 2 immunity is related to severity of bleomycin-induced lung fibrosis (Brodeur et al. 2015). Taken together, these findings suggest that eupatilin could be useful as an effective therapeutic agent against fibrosis, especially IPF.

bioRxiv preprint doi: https://doi.org/10.1101/106591; this version posted February 16, 2017. The copyright holder for this preprint (which was not certified by peer review) is the author/funder. All rights reserved. No reuse allowed without permission.

Acknowledgements

This study was supported by an intramural fund from OsteoNeuroGen. B-S Y and H-S Kim conceived the idea. H-S Yoon contributed to determining the structure-function relationship and I-H Kim coordinated the experiments and helped with writing the manuscript. J-H Kim was largely involved in executing major experiments, J Y Lee contributed to real-time imaging , and Y-M Yoon took part in high through-put screening and the EMT assay. Mice were taken care by the IACUC associated with Woojungbsc Co under IRB 13023.

Competing financial interests: H-S Kim, I-K Kim, HS Yoon, and B-S Youn retain shares of OsteoNeuroGen, and J-H Kim and Y-M Yoon are employed by OsteoNeuroGen. The anti-fibrosis capability of Chromones is the subject of a Korea patent, an international PCT, and a US patent.

bioRxiv preprint doi: https://doi.org/10.1101/106591; this version posted February 16, 2017. The copyright holder for this preprint (which was not certified by peer review) is the author/funder. All rights reserved. No reuse allowed without permission.

Materials and Methods

Establishment of the murine HSC line ONGHEPA1

Animal experiments were approved and conducted in accordance with the guidelines of the Institutional Animal Care and Use Committee at Catholic Kwandong University (IACUC No. CKU01-2015-014). C57BL/6 mice at 8 weeks of age were purchased from Charles River Orient (Seoul, Korea). The animals were housed under a 12 hr light/dark cycle at 21 ± 2°C and 50 ± 5% humidity in an environment-controlled room.

HSCs were isolated from 8-week-old C57BL/6 mice using a standard protocol for liver perfusion (Geerts et al. 2001) with minor modifications. Briefly, the liver was pre-perfused through the portal vein with PBS (Invitrogen, Carlsbad, CA, USA) containing 50 mM glucose, 100 U/ml penicillin, 100 μg/ml streptomycin, and 0.01% collagenase type IV (Sigma Chem, St. Louis, MO, USA). After excision from the body, livers were homogenized and digested for 30 min at 37°C with 0.01% collagenase type I (Sigma). The resultant cells were resuspended in ice-cold PBS containing 10% fetal bovine serum (FBS; Hyclone, Logan, UT, USA) and filtered through a 100-μm cell strainer (Sigma), followed by centrifugation at 300×*g* for 7 min. Subsequently, the cells were resuspended in PBS with 1% FBS, and then subjected to discontinuous Percoll (GE Healthcare, Piscataway, NJ, USA) gradient centrifugation at 1200 ×*g* for 30 min. Isolated cells were cultured on a tissue culture plate in DMEM with high glucose (Invitrogen) supplemented with 10% FBS and antibiotics at 37°C and 5% CO_2. After incubation, the plates were washed extensively with PBS to remove contaminating cells, and the medium was changed every 3 days. When the cells reached 70% confluence, they were

bioRxiv preprint doi: https://doi.org/10.1101/106591; this version posted February 16, 2017. The copyright holder for this preprint (which was not certified by peer review) is the author/funder. All rights reserved. No reuse allowed without permission.

passaged at a ratio of 1:3–1:5. The resultant cells, which exhibited stable morphology and doubling time even after 35 passages, were designated ONGHEPA1. Cells at passage 3–10 were used for experiments.

Cell culture and reagents

Recombinant human TGFβ and PDGF were obtained from Peprotech (Rocky Hill, CT, USA) and used at a final concentration of 5 ng/ml. Chemically synthesized eupatilin was obtained from Syngene International Ltd. (Bangalore, India), dissolved at a stock concentration of 50 mM in DMSO, and stored in aliquots at -20°C. DMSO at 0.1% (v/v) was used as a control. ONGE200 (hispidulin) and ONGA300 (jaceosidin) were purchased from AK Scientific (Union City, CA, USA). The remaining 31 CDs in the test set purchased from Analyticon (Berlin, Germany). For simultaneous treatment, ONGHEPA1 cells were seeded in 1 ml of DMEM-high glucose supplemented with 10% FBS, 100 units/ml penicillin, and 0.1 mg/ml streptomycin in 24-well plates (5.5×10^4 cells/well). After 24 hr, the wells were washed with D-PBS (Lonza), and the medium was replaced with DMEM containing 5 ng/ml TGFβ to induce fibrosis. For simultaneous treatment, eupatilin (50 μM) was added to the medium, and the samples were incubated for 24 hr. For sequential treatment, the cells were seeded in 1 ml of DMEM/10% FBS in 24-well plates (5.5×10^4 cells/well). After 24 hr, the wells were washed with PBS, and the medium was replaced with DMEM containing 5 ng/ml TGFβ. Following incubation at 37°C and 5% CO_2 for 24 hr, the medium was replaced with to DMEM containing 5 ng/ml TGFβ and 50 μM ONG2 and incubated for an additional 24 hr. The anti-fibrotic effect of eupatilin was examined under a microscope (EVO, Life Technologies).

bioRxiv preprint doi: https://doi.org/10.1101/106591; this version posted February 16, 2017. The copyright holder for this preprint (which was not certified by peer review) is the author/funder. All rights reserved. No reuse allowed without permission.

Flow cytometry

Cell pellets were suspended in PBS supplemented with 1% FBS and stained with antibodies against the following proteins: CD29, CD44, CD45, CD71, CD90, CD106, and CD117. All antibodies were obtained from BD Biosciences (San Jose, CA, USA) and conjugated with either R-PE or FITC. After incubation for 20 min at 4°C in the dark, the cells were washed, and pellets were resuspended in PBS containing 1% paraformaldehyde (BioSesang, Seongnam, Korea). Labeled cells were analyzed on a flow cytometer (Cytomics Flow cytometer, Beckman Coulter, Fullerton, CA, USA)

Cell viability assay

ONGHEPA1 cells (10^6 cells/well) were seeded in 96-well microtiter plates and incubated overnight. Cells were treated with TGFβ and the indicated concentrations of eupatilin or other CDs for 24 hr. Cell viability was measured using the CCK-8 kit (Dojindo Molecular Technologies, Japan).

Immunostaining

For immunofluorescence staining, ONGHEPA1 cells were grown on 8-well glass chamber slides (LabTek II, Thermo Fisher, Rochester, NY, USA) and fixed with methanol at -80°C for 2 hr. After washing with PBS, cells were blocked and permeabilized by incubation at room temperature for 2 hr in PBS/5% FBS with 0.1% Triton X-100. After incubation with primary antibodies at 4°C overnight, cells were washed, stained with dye-conjugated secondary antibodies, and incubated at room temperature for 2 hr. GATA4 (Santa Cruz Biotechnology, Dallas, TX, USA) and cytokeratin 18 (Santa Cruz Biotechnology) were used as markers of endoderm and endothelial cells, respectively. Nuclei were counterstained with DAPI.

bioRxiv preprint doi: https://doi.org/10.1101/106591; this version posted February 16, 2017. The copyright holder for this preprint (which was not certified by peer review) is the author/funder. All rights reserved. No reuse allowed without permission.

Live-cell imaging

ONGHEPA1 cells were seeded in DMEM supplemented with 10% FBS and 1% penicillin/streptomycin in 35-mm culture dishes (BD) at a concentration of 5×10^4 cells/well. After overnight culture, cells were washed with PBS, and the medium was replaced with serum-free DMEM medium with recombinant TGFβ (5 ng/ml, Peprotech) or ONG2 (50 μM). Immediately thereafter, cells with clear morphology were identified by observation in the differential interference contrast channel, and analysis was performed in an insulated chamber (TC-L-10; incubator system, Korea) maintained at 37°C, 5% CO_2. A series of bright-field images was collected every 5 min over 24 hr period on an Olympus IX73 inverted microscope using a 10× objective. Image stacks were converted to AVI formats using cellSens imaging software (Olympus).

Reverse transcriptase PCR and real-time PCR

Cells cultured in 24-well plates were harvested with Trypsin-EDTA solution (Welgene, Seoul, Korea). Specifically, the wells were washed once with DPBS, and then 1× Trypsin-EDTA solution was added to each well and incubated for 2–3 minutes. Trypsin-EDTA solution was inactivated by DMEM containing 10% of FBS. The resultant cell suspensions were transferred to 1.5-ml cap tubes, which were centrifuged for 5 minutes at 800×g. After centrifugation, the supernatant was removed, and the pellets were washed once with DPBS. Total RNA was purified from the pellets using the RNeasy mini Kit (Qiagen). The concentration of purified RNA was measured using a Multiskan GO and μDrop plate (Thermo). RNA was reverse-transcribed using the cDNA Synthesis Kit (PCRBio). Reverse transcriptase was activated by incubation at 42°C for 30 minutes, and then denatured at 85°C for 10 minutes. Synthesized cDNA was amplified with StepOne Plus (Applied Biosystems) and 2× qPCRBio Probe Mix

bioRxiv preprint doi: https://doi.org/10.1101/106591; this version posted February 16, 2017. The copyright holder for this preprint (which was not certified by peer review) is the author/funder. All rights reserved. No reuse allowed without permission.

Hi-ROX (PCRBio). PCR conditions were as follows: by polymerase activation for 2 minutes at 95°C, followed by 40 cycles of denaturation at 95°C for 5 seconds and annealing/extension at 62°C for 25 seconds. Comparisons between mRNA levels genes were performed using the ΔΔCt method, with *Gapdh* as the internal control.

RNA-Seq processing, differential gene expression analysis, and interactome analysis

For preprocessing of total sequencing reads, adapter trimming was performed using cutadapt with default parameters, and quality trimming (Q30) was performed using FastQC with default parameters. Processed reads were mapped to the *Mus musculus* reference genome (Ensembl 77) using tophat and cufflink with default parameters (Trapnell et al. 2012). Differential analysis was performed using Cuffdiff (Trapnell et al. 2012) using default parameters. Further, the FPKM values from Cuffdiff were normalized and quantitated using the R Package Tag Count Comparison (TCC) (Sun et al. 2013) to determine statistical significance (e.g., P values) and differential expression (e.g., fold changes). Gene expression values were plotted in various ways (i.e., Scatter, MA, and Volcano plots), using fold-change values, with an R script developed in-house. To compare individuals and combinations of samples, unique regulated genes were subjected to Venn diagram analysis (http://bioinformatics.psb.ugent.be/webtools/Venn/). The protein interaction transfer procedure was performed by the STRING database (Szklarczyk et al. 2011) with the differentially expressed genes. The highest-confidence interaction score (0.9) was applied from the *Mus musculus* species, and information about interacts were obtained based on text mining, experiments, and databases (http://www.string-db.org/).

Evaluation of effect on fibrosis of lung tissue induced by bleomycin

Five-week-old male C57BL/6J mice (body weight: 18.2–20.5 g) (KOATECH, Korea) were

bioRxiv preprint doi: https://doi.org/10.1101/106591; this version posted February 16, 2017. The copyright holder for this preprint (which was not certified by peer review) is the author/funder. All rights reserved. No reuse allowed without permission.

used for experiments, and each test group was composed of five animals, as summarized in Table 1. The mice were housed in breeding boxes with dimensions of 369 (L) × 156 mm (W) × 132 mm (H) (EU, USA, UK GL compliance) made of a polysulfone material in a SPF (Specific Pathogen–Free) and BSL (Bio Safety Level) 2 grade facility. Two or three animals were present in each breeding box during the period of quarantine and acclimatization, as well as during the testing period, and the conditions were set to a temperature of 22 ± 2°C, a relative humidity of 50.0 ± 15.0%, a ventilation cycle of 10–20 times/hr, a light/dark cycle (photoperiod) of 12 hr/day (07:00 to 19:00), and illumination intensity of 150–300 Lux during the light phase. Pulmonary fibrosis was induced by directly injecting bleomycin solution into the lungs according to the intratracheal instillation (IT) method of Kremer, Laxer and Berkman *et al*. Briefly, C57BL/6J mice were anesthetized by inhalation of 70% N_2O and 30% O_2 gas containing 1.5% isoflurane; the skin of the anterior neck thereof was excised, and the tissues under the muscle were exposed and carefully incised using ophthalmic surgical scissors. Fifty microliters of bleomycin solution in distilled water was directly injected into the lungs all at once via the aperture created by excision of tissue using a 1-ml syringe fitted with a 19-gauge injection needle with a blunt tip. Immediately after injection, the incised skin of the anterior neck was sutured, and the mice were allowed to recover from the anesthetic, transferred into a general breeding cage, and then bred. Bleomycin-HCl (40 μg/50 μl) was administered once using a visual instillobot. Eupatilin was dissolved in DPBS buffer (containing 1% DMSO), and 1 ml/kg was administered based on the most recent body weight. Twelve days after the administration of bleomycin, eupatilin was forcibly nasally administered via a micropipette, once a day (five times a week) for 1 week. For 2 to 3 days after the administration of eupatilin, mice were monitored for toxic symptoms or death, but no abnormal symptoms were observed. Three mice per test group were selected, and their

bioRxiv preprint doi: https://doi.org/10.1101/106591; this version posted February 16, 2017. The copyright holder for this preprint (which was not certified by peer review) is the author/funder. All rights reserved. No reuse allowed without permission.

lung tissues were excised. The lung tissues were stained with Masson's trichrome and observed under a microscope. Results were demonstrated by mean values and standard deviations. Controls and eupatilin-treated mice data were subjected to ANOVA analysis. Statistic meaning was considered positive when 5% differences between samples were pronounced. Fisher's PLSD was conducted for confirmation of statistical significane.

bioRxiv preprint doi: https://doi.org/10.1101/106591; this version posted February 16, 2017. The copyright holder for this preprint (which was not certified by peer review) is the author/funder. All rights reserved. No reuse allowed without permission.

REFERENCES

Andrae J, Gallini R, Betsholtz C. 2008. Role of platelet-derived growth factors in physiology and medicine. Genes Dev.22:1276-1312.

Bonnans C, Chou J, Werb Z. 2014. Remodelling the extracellular matrix in development and disease. Nat Rev Mol Cell Biol.15:786-801.

Brodeur TY, Robidoux TE, Weinstein JS, Craft J, Swain SL, Marshak-Rothstein A. 2015. IL-21 Promotes Pulmonary Fibrosis through the Induction of Profibrotic CD8+ T Cells. J Immunol.195:5251-5260.

Dixon RA, Pasinetti GM. 2010. Flavonoids and isoflavonoids: From plant biology to agriculture and neuroscience. Plant Physiol.154:453-457.

Dong Y, Geng Y, Li L, Li X, Yan X, Fang Y, Li X, Dong S, Liu X, Li X, et al. 2015. Blocking follistatin-like 1 attenuates bleomycin-induced pulmonary fibrosis in mice. J Exp Med 212:235-252.

Emami S, Ghanbarimasir Z. 2015. Recent advances of chroman-4-one derivatives: synthetic approaches and bioactivities. Eur J Med Chem 93:539-563.

Fallowfield JA. 2015. Future mechanistic strategies for tackling fibrosis--an unmet need in liver disease. Clin Med (Lond).15 Suppl.:s83-s87.

Gabele E, Brenner DA, Rippe RA. 2003. Liver fibrosis: signals leading to the amplification of the fibrogenic hepatic stellate cell. Front Biosci.8:d69-d77.

Gacche RN, Meshram RJ, Shegokar HD, Gond DS, Kamble SS, Dhabadge VN, Utage BG, Patil KK, More RA. 2015. Flavonoids as a scaffold for development of novel anti-angiogenic agents: An experimental and computational enquiry. Arch Biochem Biophys 577-578:35=48.

Geerts A, Eliasson C, Niki T, Wielant A, Vaeyens F, Pekny M. 2001. Formation of normal

bioRxiv preprint doi: https://doi.org/10.1101/106591; this version posted February 16, 2017. The copyright holder for this preprint (which was not certified by peer review) is the author/funder. All rights reserved. No reuse allowed without permission.

desmin intermediate filaments in mouse hepatic stellate cells requires vimentin. Hepatol.33:177-188.

Huang SK, Scruggs AM, McEachin RC, White ES, Peters-Golden M. 2014. Lung fibroblasts from patients with idiopathic pulmonary fibrosis exhibit genome-wide differences in DNA methylation compared to fibroblasts from nonfibrotic lung. PLoS One.12:e107055.

Ji HY, Kim SY, Kim DK, Jeong JH, Lee HS. 2010. Effects of eupatilin and jaceosidin on cytochrome p450 enzyme activities in human liver microsomes. Molecules.15:6466-6475.

Kim JY, Lee MS, Bae JM, Park J, Youn BS, J O. 2015. Massive elimination of multinucleated osteoclasts by eupatilin is due to dual inhibition of transcription and cytoskeletal rearrangement. Bone Rep.3:83-94.

King CS, Nathan SD. 2015. Practical considerations in the pharmacologic treatment of idiopathic pulmonary fibrosis. Curr Opin Pulm Med 21:479-489.

Lamouille S, Xu J, Derynck R. 2014. (Molecular mechanisms of epithelial–mesenchymal transition. Nat Rev Mol Cell Biol.15:178-196.

Leyva-López N, Gutierrez-Grijalva EP, Ambriz-Perez DL, Heredia JB. 2016. Flavonoids as cytokine modulators: A possible therapy for inflammation-related diseases. Int J Mol Sci 17:921.

Lovisa S, LeBleu VS, Tampe B, Sugimoto H, Vadnagara K, Carstens JL, Wu CC, Hagos Y, Burckhardt BC, Pentcheva-Hoang T, et al. 2015. Epithelial-to-mesenchymal transition induces cell cycle arrest and parenchymal damage in renal fibrosis. Nat Med.21:998-1009.

Murray LA. 2016. The cell types of fibrosis. Front Pharmacol.6:311.

Poynard T, Lebray P, Ingiliz P, Varaut A, Varsat B, Ngo Y, Norha P, Munteanu M, Drane F, Messous D, et al. 2010. Prevalence of liver fibrosis and risk factors in a general population using non-invasive biomarkers (FibroTest). BMC Gastroenterol.10:40.

bioRxiv preprint doi: https://doi.org/10.1101/106591; this version posted February 16, 2017. The copyright holder for this preprint (which was not certified by peer review) is the author/funder. All rights reserved. No reuse allowed without permission.

Sgalla G, Cocconcelli E, Tonelli R, Richeldi L. 2016. Novel drug targets for idiopathic pulmonary fibrosis. Expert Rev Respir Med.26:1-13.

Stapleton AE, Walbot V. 1994. Flavonoids can protect maize DNA from the induction of ultraviolet radiation damage. Plant Physiol.105:881-889.

Sun J, Nishiyama T, Shimizu K, Kadota K. 2013. TCC: an R package for comparing tag count data with robust normalization strategies. BMC Bioinformatics.14:219.

Szklarczyk D, Franceschini A, Kuhn M, Simonovic M, Roth A, Minguez P, Doerks T, Stark M, Muller J, Bork P, et al. 2011. The STRING database in 2011: functional interaction networks of proteins, globally integrated and scored. Nucleic Acids Res 39:D561-568.

Trapnell C, Roberts A, Goff L, Pertea G, Kim D, Kelley DR, Pimentel H, Salzberg SL, Rinn JL, Pachter L. 2012. Differential gene and transcript expression analysis of RNA-seq experiments with TopHat and Cufflinks. Nat Protoc.7:562-578.

bioRxiv preprint doi: https://doi.org/10.1101/106591; this version posted February 16, 2017. The copyright holder for this preprint (which was not certified by peer review) is the author/funder. All rights reserved. No reuse allowed without permission.

Figure Legends

Figure 1. Inhibition of TGFβ- or PDGF-induced fibrosis by eupatilin

A) ONGHEPA1 cells were stimulated with TGFβ (5 ng/ml) or TGFβ plus eupatilin (50 μM) for 24 hr, and morphological changes were monitored under a light microscope. ICC was performed using anti-mouse α smooth muscle actin B) ONGHEPA1 cells were stimulated with PDGF (5 ng/ml) or PDGF plus eupatilin (50 μM) for 24 hr, and morphological changes were monitored under a light microscope. ICC was conducted as described above. C) ONGHEPA1 cells were grown to confluence, washed, and maintained overnight in serum-free medium. The cells were then treated with TGFβ or TGFβ plus eupatilin for the indicated times, and fibrosis was monitored.

Figure 2. Inhibition of fibrogenesis of normal human lung fibroblasts (NHLF) by CDs

NHLF cells ($5X10^6$) were seeded in fibroblast growth medium (FBM), grown overnight, and then stimulated with controls or CDs for 48 hr or 72hr.

A) NHLF cells were simultaneously stimulated with TGFβ or TGFβ plus eupatilin (50μM), ONGE200 (50μM), or ONGA300 (10μM). Anti-fibrosis was assessed by light microscopy.

B) Total RNAs were isolated from NHLF cell stimulated with FBM, TGFβ , or TGFβ plus eupatilin for 48 hr or 72 hr and were subjected to real-time PCR analysis. Standard deviations were calculated from the results of three independent PCRs.

bioRxiv preprint doi: https://doi.org/10.1101/106591; this version posted February 16, 2017. The copyright holder for this preprint (which was not certified by peer review) is the author/funder. All rights reserved. No reuse allowed without permission.

Figure 3. Differential effects of chemical moieties of the chromone scaffold on the anti-fibrotic capacity of CDs

A and C) Chromone scaffold and chemical moieties of eupatilin and ONGI300. The sole difference in the chemical moieties of these CDs is marked by a blue box. ONGHEPA1 cells were simultaneously stimulated with TGFβ, TGFβ plus eupatilin, or TGFβ plus ONGI300 at the indicated doses. Anti-fibrotic capacities were observed by light microscopy.

B and E) Chromone scaffold and chemical moieties of ONGE200 (hispidulin) and ONGI200 (apigenin). C6, which is methoxylated, is indicated by a red letter. Hydroxy groups shared between these CDs are represented by a red box. ONGHEPA1 cells were simultaneously stimulated with TGFβ, TGFβ plus ONGE200, or TGFβ plus ONGI300 at the indicated doses. Anti-fibrotic capacities were observed by light microscopy.

C and F) Chromone scaffold and chemical moieties of ONGA300 (jaceosidin) and ONGH300. The exclusively difference, methoxylation at C2, is indicated by a yellow letter. Methoxy and hydroxy groups shared between these CD members are represented by purple boxes. ONGHEPA1 cells were simultaneously stimulated with TGFβ, TGFβ plus ONGA300 or TGFβ plus ONGH200 at the indicated doses. Anti-fibrotic capacities were observed by light microscopy.

Figure 4. Structure–activity relationship of a selected group of chromone derivatives (CDs).

The structure–activity relationships of chromone compounds with similar chemical structures

bioRxiv preprint doi: https://doi.org/10.1101/106591; this version posted February 16, 2017. The copyright holder for this preprint (which was not certified by peer review) is the author/funder. All rights reserved. No reuse allowed without permission.

are summarized. To determine their biological effects, ONGHEPA1 cells were treated with TGFβ for 24 hr in the absence or presence of the indicated compounds. Anti-fibrotic activities were monitored by light microscopy. Three chromones (eupatilin, ONGE200, and ONGA300) exhibited anti-fibrotic activities. R1 and R2 are common in most chromones. Substitutions of R3 and R4 exhibit little toleration for their anti-fibrotic activities, suggesting that the functional groups are important for the anti-fibrotic effects mediated by chromone compounds. OMe, Methoxy group.

Figure 5. TGFβ stimulation is essential for the anti-fibrotic activity of selected CDs

A) ONGHEPA1 cells were differentiated into myofibroblasts in the presence of medium, DMSO, eupatilin alone, TGFβ alone, or TGFβ plus eupatilin. Anti-fibrotic capacities were assessed by light microscopy.

B) ONGHEPA1 cells were pre-stimulated with eupatilin for 2, 4, or 6 hr, washed, and then stimulated with TGFβ for 24 hr.

C) ONGHEPA1 cells were stimulated for the indicated times with TGFβ, washed, and then stimulated with TGFβ plus eupatilin for 24 hr.

Figure 6. Reversal of fibrosis by selected CDs correlates with inhibition of EMT

A) ONGHEPA1 cells were stimulated with TGFβ for 24 hr to achieve full differentiation of the fibroblasts. The cells were then washed and re-stimulated for 24 hr with TGFβ, TGFβ plus eupatilin, or TGFβ plus ONGE200. Morphological changes were observed

bioRxiv preprint doi: https://doi.org/10.1101/106591; this version posted February 16, 2017. The copyright holder for this preprint (which was not certified by peer review) is the author/funder. All rights reserved. No reuse allowed without permission.

by light microscopy.

B) ONGHEPA1 cells were stimulated with PDGF for 24 hr, washed, and re-stimulated for 24 hr with PDGF, PDGF plus eupatilin, or PDGF plus ONGE200.

C-D) Real-time PCR experiments were conducted using a set of TaqMan primers corresponding to *Col11a1*, *Slit3* (slit homolog 3 Drosophila), *Axl* (receptor tyrosine kinase), *Postn* (periostin), *Fn1* (fibronectin 1) and *Aurka* (Aurora kinase). Standard deviations were calculated from the results of three independent PCRs.

Figure 7. Comparison of anti-fibrotic features between simultaneous and sequential stimulation with selected CDs

A) Chromone scaffold and the dimethoxy residues of eupatilin are depicted by carbon numbers and a blue box, respectively. ONGHEPA1 cells were simultaneously stimulated for 24 hr with TGFβ or PDGF in the presence of eupatilin. Reversal of fibroblast morphology was observed under light microscope. ONGHEPA1 cells were sequentially stimulated for 24 hr with TGFβ, followed by re-stimulation for 24 hr with TGFβ or TGFβ plus eupatilin. Morphological changes were observed by light microscopy.

B and C) ONGE200 and ONGA300 were employed for simultaneous and sequential stimulation described above for eupatilin.

Figure 8. An interactome generated by simultaneous stimulation of ONGHEPA1 cells

bioRxiv preprint doi: https://doi.org/10.1101/106591; this version posted February 16, 2017. The copyright holder for this preprint (which was not certified by peer review) is the author/funder. All rights reserved. No reuse allowed without permission.

with TGFβ and eupatilin reveals an EMT-related pathway

Total RNAs were isolated from TGFβ-treated or TGFβ plus eupatilin–treated ONGHEPA1 cells. One microgram of RNA from each ample was subjected to RNA-Seq, yielding a total of 60Gb of sequence, and gene interactions were established as described in Materials and Methods. Regulated genes were selected below $p<0.05$. Eight hubs are represented by colored boxes or ovals, and critical nodes are depicted as purple ovals.

Figure 9. Administration of eupatilin to bleomycin-treated mice significantly improves lung fibrosis

Bleomycin, vehicle, or various concentrations of eupatilin (5–40 μg) were intratracheally injected into C57BL/6J mice for 12 days. Bleomycin injection gave a rise to fulminant fibrosis in all mice receiving the drug. Eupatilin was dissolved in DPBS buffer (containing 1% DMSO) and administered nasally for 6 days. Three mice per test group were selected, and their lung tissues were excised. The lung tissues were stained with Masson's trichrome and observed under a microscope. Blood leukocytes were isolated and counted.

bioRxiv preprint doi: https://doi.org/10.1101/106591; this version posted February 16, 2017. The copyright holder for this preprint (which was not certified by peer review) is the author/funder. All rights reserved. No reuse allowed without permission.

Supplementary Figure Legends

Suppl. Fig. 1. (A) Lists of downregulated genes associated with EMT in eupatilin-treated osteoclasts. (B) Morphology of the mouse HSC line, ONGHEPA1. (phase-contrast microscopy; ×40 magnification, scale bars = 200 μm). (C) Immunophenotype of ONGHEPA1. Immunofluorescence staining of GATA4 and Cytokeratin 18. Nuclei were counterstained with DAPI. (×200 magnification; scale bar = 500 μm).

Suppl. Fig. 2. Phenotypic changes in ONGHEPA1 cells treated with TGFβ

Phase-contrast images of TGFβ-treated ONGHEPA1 cells taken at the indicated time points during a 48-hr culture (×100 magnification).

Suppl. Fig. 3. Chemical synthesis of eupatilin

Eupatilin was synthesized in a seven-step synthesis and purified to homogeneity according to GLP standards. Selective benzylation of chrysin (1) followed by methylation gave protected chrysin (2). Base-mediated fragmentation of (2) yielded the acetophenone (3). The hydroxyl group was introduced by Elbs persulfate oxidation followed by methylation, and aldol condensation with 3,4-dimethoxybenzaldehyde afforded the chalcone (6). Cyclization of (6) using SeO_2 in refluxing isoamyl alcohol provided the flavone derivative (7), which upon deprotection of the benzyl group, followed by de-methylation, yielded eupatilin.

bioRxiv preprint doi: https://doi.org/10.1101/106591; this version posted February 16, 2017. The copyright holder for this preprint (which was not certified by peer review) is the author/funder. All rights reserved. No reuse allowed without permission.

Suppl. Fig. 4. Phenotypic changes in ONGHEPA1 cells treated with PDGF

Phase-contrast images of PDGF-treated ONGHEPA1 cells, taken at the indicated time points during 24-hr culture (×100 magnification).

Suppl. Fig. 5 Inhibition of fibrogenesis of normal human lung fibroblasts (NHLF) by CDs.

NHLF cells ($5X10^6$) were seeded in fibroblast growth medium (FBM), grown overnight, and stimulated with CDs or corresponding controls for 48 hr or 72hr

A) NHLF cells were simultaneously stimulated with TGFβ or TGFβ plus eupatilin and were subjected to ICC using anti-human α smooth muscle actin.

B) NHLF cells were simultaneously stimulated with PDGF or PDGF plus eupatilin (50μM), ONGE200 (50μM), or ONGA300 (10μM). Anti-fibrosis was assessed by light microscopy.

C) Total RNAs were isolated from NHLF cell stimulated with FBM, PDGF or PDGF plus eupatilin for 48 hr or 72 hr and were subjected to real-time PCR analysis. Standard deviations were calculated from the results of three independent PCRs.

B) **Suppl. Fig. 6** Real-time imaging of morphological changes of ONGHEPA1 cells upon stimulation with TGFβ or simultaneous stimulation with TGFβ plus eupatilin A) ONGHEPA1 cells were stimulated with TGFβ and their differentiation was assessed by 24 hr real-time imaging. ONGHEPA1 cells were simultaneously stimulated with TGFβ and eupatilin and anti-fibrosis was assessed for 24 hr. Frames were acquired

bioRxiv preprint doi: https://doi.org/10.1101/106591; this version posted February 16, 2017. The copyright holder for this preprint (which was not certified by peer review) is the author/funder. All rights reserved. No reuse allowed without permission.

every 5 minutes for 24 hr using live-cell imaging.

Suppl. Fig. 7. Representation of the 34 CDs used in the anti-fibrotic assay

Groupings were established based on chemical moieties bonded to the chromone scaffold or linked to the adjacent phenyl group. Generic names are indicated by blue letters.

Suppl. Fig. 8-1 and 8-2. Representation of anti-fibrotic capacity exhibited by the 34 CDs

ONGHEPA1 cells were simultaneously stimulated with TGFβ or TGFβ plus each CD, and inhibition of fibrosis was assessed by phase-contrast microscopy. A blue circle represents ONGC200, which contains a methoxy group at C7. Concentration-dependent anti-fibrotic assay was conducted with ONGD400, which has a methoxy group at C2 and exhibits strong cytotoxicity. ONGH300 and ONGD400 are stereoisomers that differ by a hydroxy group and a methoxy group coupled to the phenyl group.

Suppl. Fig. 9-1 and 9-2, Anti-fibrotic capacities of the 34 CDs upon sequential stimulation of ONGHEPA1 cells with TGFβ+CDs

ONGHEPA1 were stimulated with TGFβ for 24 hr, washed, and re-stimulated with the indicated CDs. Anti-fibrotic capacities were observed by light microscopy. Generic CDs are denoted by blue letters.

bioRxiv preprint doi: https://doi.org/10.1101/106591; this version posted February 16, 2017. The copyright holder for this preprint (which was not certified by peer review) is the author/funder. All rights reserved. No reuse allowed without permission.

Suppl. Fig. 10-1 and 10-2. Anti-fibrotic capacities of the 34 CDs upon sequential stimulation of ONGHEPA1 with PDGF+CDs

ONGHEPA1 were stimulated with PDGF for 24 hr, washed, and re-stimulated with CDs. Anti-fibrotic capacities were observed by light microscopy. Generic CDs are denoted by blue letters.

Suppl. Fig. 11 Real-time imaging of morphological reversion of TGFβ-treated ONGHEPA1 cells after sequential stimulation with TGFβ and eupatilin

A) ONGHEPA1 cells were stimulated with TGFβ for 48 hr and their differentiation was assessed by real-time imaging

B) ONGHEPA1 cells were stimulated with TGFβ for full differentiation into myofibroblasts for 24 hr, washed with PBS, and restimulated with TGFβ plus eupatilin for 24 hr. Anti-fibrosis was assessed with real-time imaging. Frames were acquired every 5 minutes for 24 hr using live-cell imaging.

Suppl. Fig. 12. Global gene expression changes between cells treated with TGFβ and those treated with TGFβ plus eupatilin

A) Volcano plot. The x-axis represents fold change ($\log_2$), and the y-axis depicts p-value.

B) RNA-Seq analysis revealed that the total number of transcripts in unstimulated ONGHEPA1, TGFβ-stimulated ONGHEPA1, and TGFβ plus eupatilin–stimulated

bioRxiv preprint doi: https://doi.org/10.1101/106591; this version posted February 16, 2017. The copyright holder for this preprint (which was not certified by peer review) is the author/funder. All rights reserved. No reuse allowed without permission.

ONGHEPA1 were 10,020, 10,030, and 10,028, respectively. TGFβ-inducible and eupatilin-repressible genes are represented by a Venn diagram.

bioRxiv preprint doi: https://doi.org/10.1101/106591; this version posted February 16, 2017. The copyright holder for this preprint (which was not certified by peer review) is the author/funder. All rights reserved. No reuse allowed without permission.

Suppl. Table 1. Changes in global gene expression and molecular targets upon simultaneous stimulation with TGFβ and eupatilin

ONGHEPA1 cells were simultaneously stimulated for 24 hr with TGFβ or TGFβ plus eupatilin. Total RNA was isolated and subjected to RNA-Seq. Sample correlation and Gene Ontology analyses were performed.

Suppl. Table 2. Changes in global gene expression and molecular targets upon sequential stimulation with TGFβ, followed by eupatilin

ONGHEPA1 cells were sequentially stimulated with TGFβ for 24 hr, or TGFβ for 24 hr followed by eupatilin for 24 hr. Total RNAs were isolated and subjected to RNA-Seq. Sample correlation and Gene Ontology analyses were performed.

Suppl. Table 3. TGFβ/eupatilin-regulated protein interactome

Eight major interactome hubs and major protein nodes are represented.

Suppl. Table 4. The 103 genes most strongly repressed by eupatilin treatment

The genes exhibiting maximal upregulation by TGFβ but maximal downregulation by eupatilin are shown.

Suppl. Table 5. Experimental setup for the treatment of mice with bleomycin or bleomycin

bioRxiv preprint doi: https://doi.org/10.1101/106591; this version posted February 16, 2017. The copyright holder for this preprint (which was not certified by peer review) is the author/funder. All rights reserved. No reuse allowed without permission.

plus increasing amounts of eupatilin

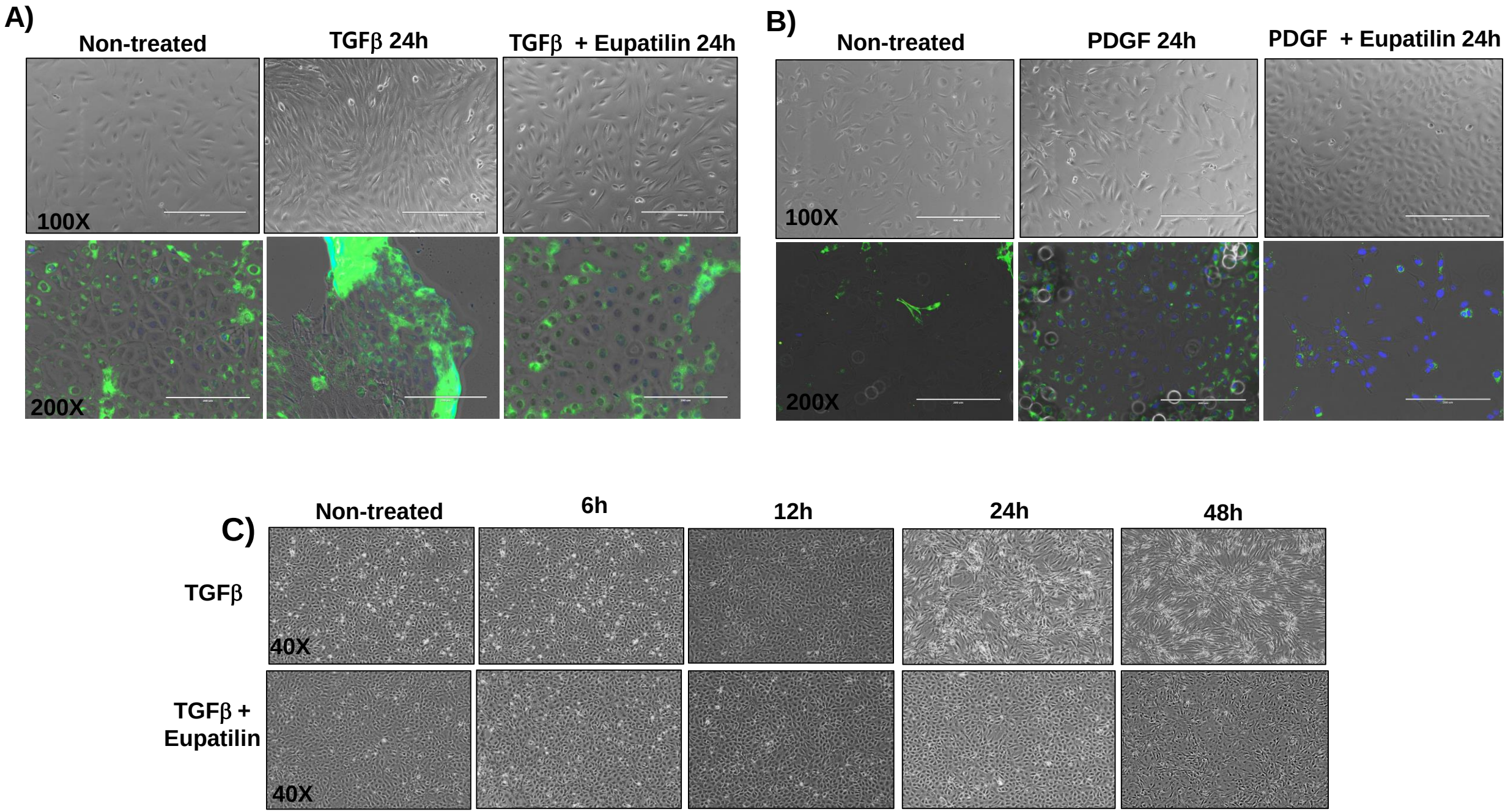
A)
Non-treated
TGFβ 24h
TGFβ + Eupatilin 24h
100X
200X
B)
Non-treated
PDGF 24h
PDGF + Eupatilin 24h
100X
200X
C)
Non-treated
6h
12h
24h
48h
TGFβ
TGFβ + Eupatilin
40X
40X

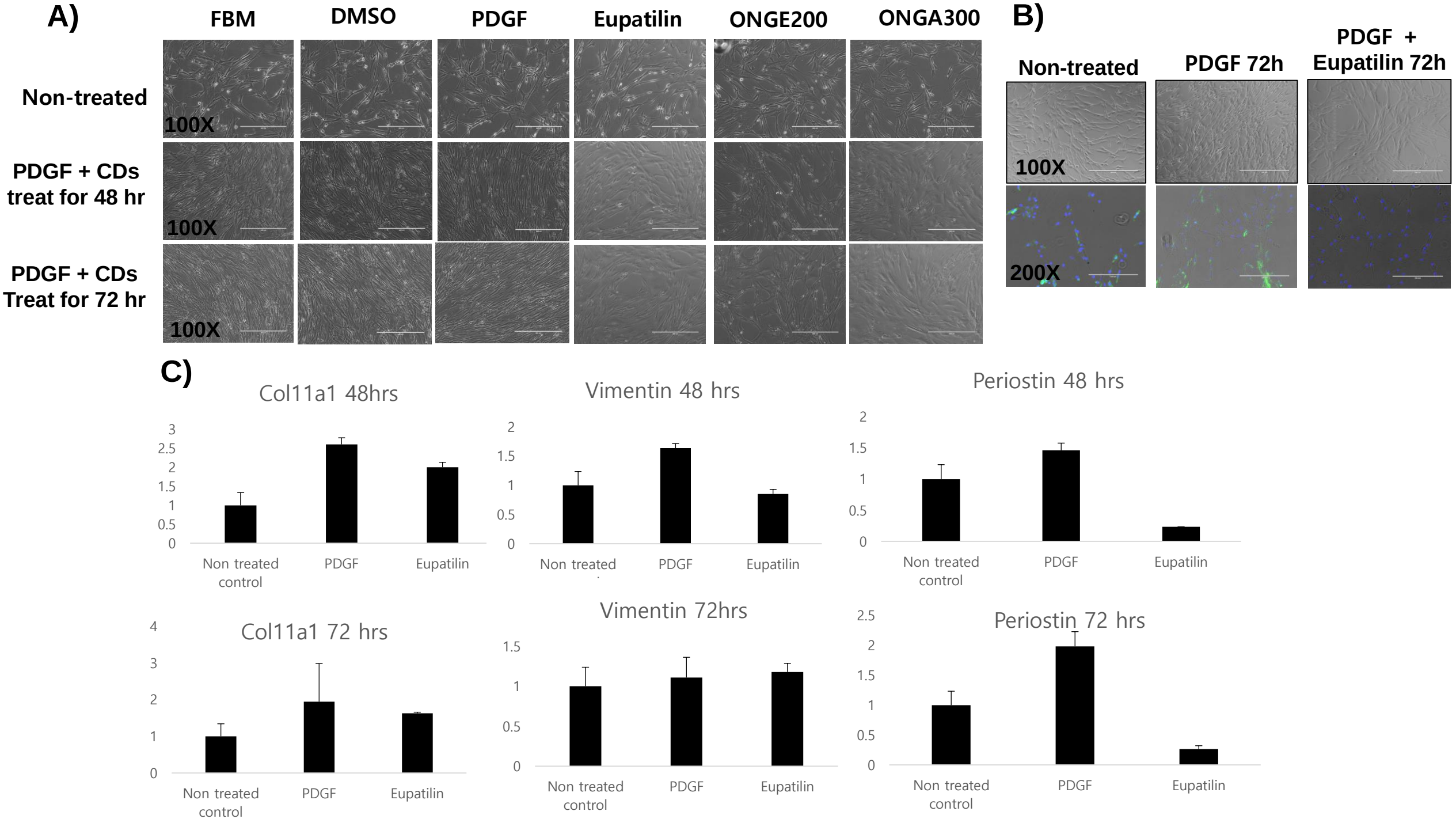
A)
FBM
DMSO
PDGF
Eupatilin
ONGE200
ONGA300
Non-treated
PDGF + CDs treat for 48 hr
PDGF + CDs Treat for 72 hr
100X
B)
Non-treated
PDGF 72h
PDGF + Eupatilin 72h
100X
200X
C)
Col11a1 48hrs
Vimentin 48 hrs
Periostin 48 hrs
Col11a1 72 hrs
Vimentin 72hrs
Periostin 72 hrs
Non treated control
PDGF
Eupatilin

A)

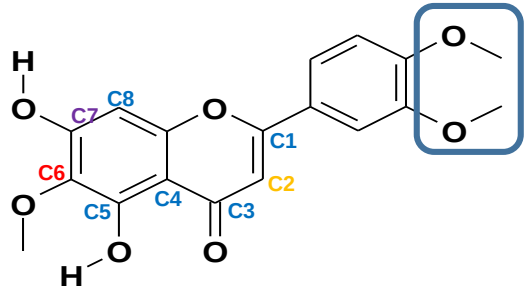

2-(3,4-dimethoxyphenyl)-5,7-dihydroxy-6-methoxy-4H-chromen-4-one (**Eupatilin**)

Non-treated	TGF-β	50μM	25μM	10μM

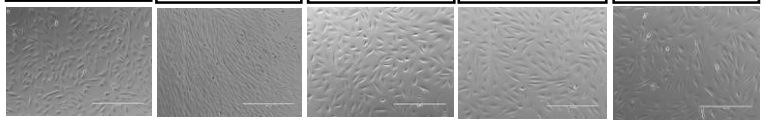

B)

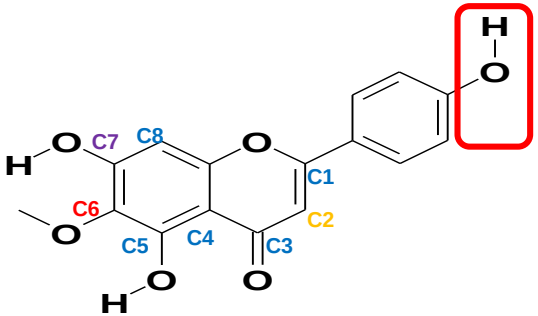

5,7-dihydroxy-2-(4-hydroxyphenyl)-6-methoxy -4H-chromen-4-one **(ONGE200) (Hispidulin)**

Non-treated	TGF-β	50μM	25μM	10μM

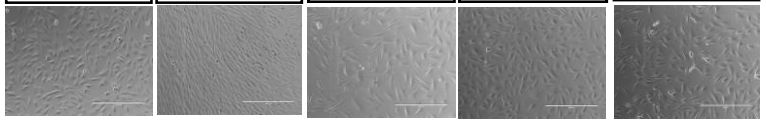

c)

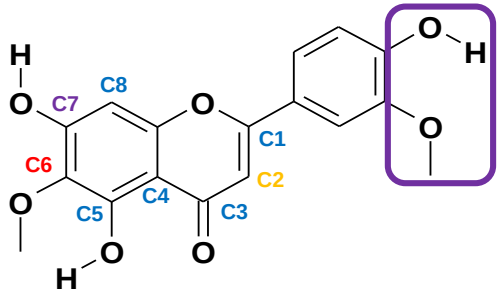

5,7-dihydroxy-2-(4-hydroxy-3-methoxyphenyl)-6-methoxy-4H-chromen-4-one (**ONGA300**)(**Jaceosidin**)

Non-treated	TGF-β	50μM	25μM	10μM

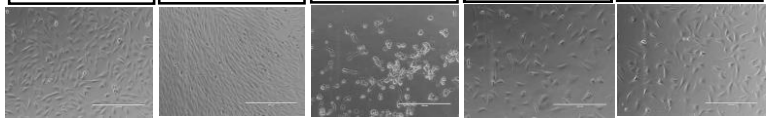

D)

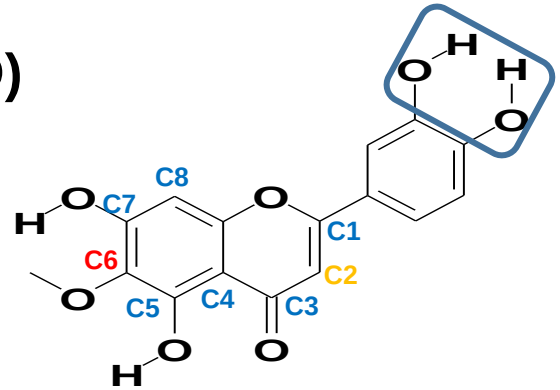

2-(3,4-dihydroxyphenyl)-5,7-dihydroxy-6-m ethoxy-4H-chromen-4-one (**ONGI300**)

Non-treated	TGF-β	50μM	25μM	10μM

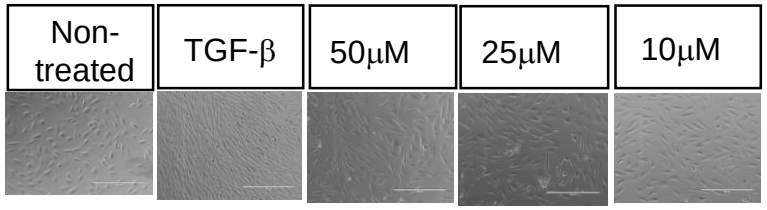

E)

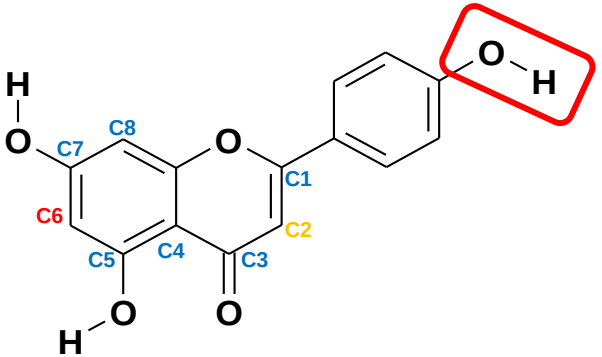

5,7-dihydroxy-2-(4-hydroxyphenyl)-4H-chromen-4-one (**ONGI200**)(**Apigenin)**

Non-treated	TGF-β	50μM	25μM	10μM

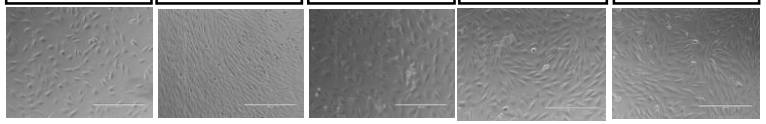

F)

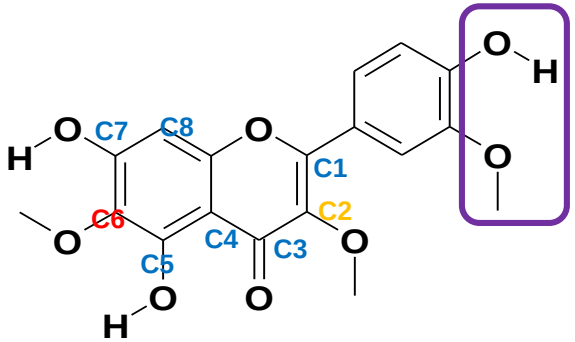

3,6-dimethoxy-4H-chromen-4-one 5,7-dihydroxy-2-(4-hydroxy-3-methoxyphenyl (**ONGH300**)

Non-treated	TGF-β	50μM	25μM	10μM

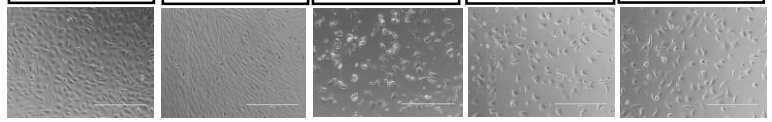

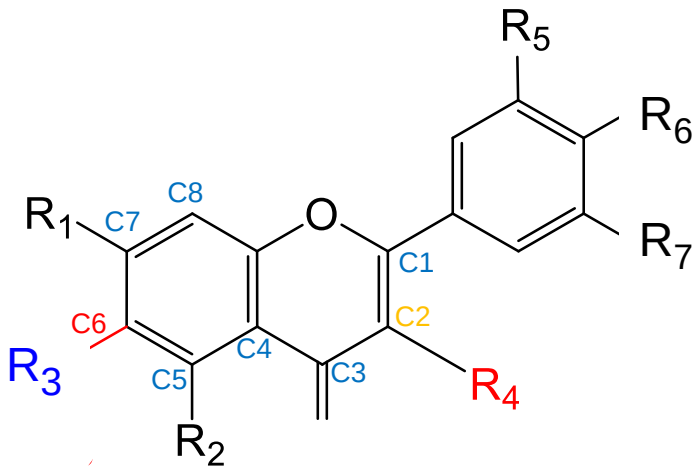

	Compound	R1	R2	R3	R4	R5	R6	R7	Anti-Fibrosis
	Eupatilin	OH	OH	OMe	H	H	OMe	OMe	++++
Group A	ONGE200	OH	OH	OMe	H	H	OH	H	+++
Group A	ONGA300	OH	OH	OMe	H	H	OH	OMe	++
Group A	ONGI300	OH	OH	OMe	H	OH	OH	H	-
Group B	ONGG200	OH	OH	H	H	H	H	H	-
Group B	ONGF300	OH	OH	OMe	OMe	H	H	H	-
Group B	ONGH300	OH	OH	OMe	OMe	H	OH	OMe	-
Group B	ONGB400	OH	OH	OMe	H	H	OMe	H	-
Group B	ONGD400	OH	OH	OMe	OMe	H	OMe	OH	-
Group B	ONGA100	OH	OH	H	OMe	H	H	H	-
Group B	ONGG100	OH	OH	H	OH	H	OH	OH	-
Group B	ONGC300	OMe	OMe	OMe	H	H	OMe	H	-
Group B	ONGG300	OMe	OH	OMe	OMe	H	OH	OH	-
Group C	ONGH100	OMe	OH	OH	H	H	H	H	-
Group C	ONGC200	OMe	OH	OMe	H	H	OH	H	-
Group C	ONGD200	OH	OH	OH	H	H	OMe	H	-
Group C	ONGH200	OMe	OH	OMe	H	OH	OH	H	-
Group C	ONGE400	OMe	OH	OMe	H	H	H	H	-
Group C	ONGG400	OMe	OMe	OMe	H	H	OMe	H	-
Group D	ONGC100	OH	H	H	H	H	OH	H	-
Group D	ONGE100	H	OMe	OH	H	H	H	H	-
Group D	ONGF200	H	H	OMe	H	H	H	H	-
Group D	ONGB300	OH	H	H	H	OH	OH	H	-
Group D	ONGD300	H	H	H	H	H	H	H	-
Group D	ONGA400	OH	H	H	H	H	H	H	-
Group D	ONGF400	H	OH	H	H	H	H	H	-
Group D	ONGE300	OH	OH	H	H	H	OH	OH	-
Group D	ONGH400	H	H	H	H	H	OMe	H	-
Group D	Apigenin	OH	OH	H	H	H	OH	H	-
Group E	ONGB100	OH	OH	H	H	H	H	H	-
Group E	ONGB200	OH	OH	H	OMe	H	OH	H	-
Group E	ONGA200	OMe	OH	H	OMe	OMe	OMe	OH	-
Group E	ONGD100	OH	OH	H	OH	OH	OH	OH	-
Group E	ONGF100	OH	OH	H	OH	H	OH	H	-
Group E	ONGC400	OMe	OMe	H	H	H	OMe	OMe	-

A)

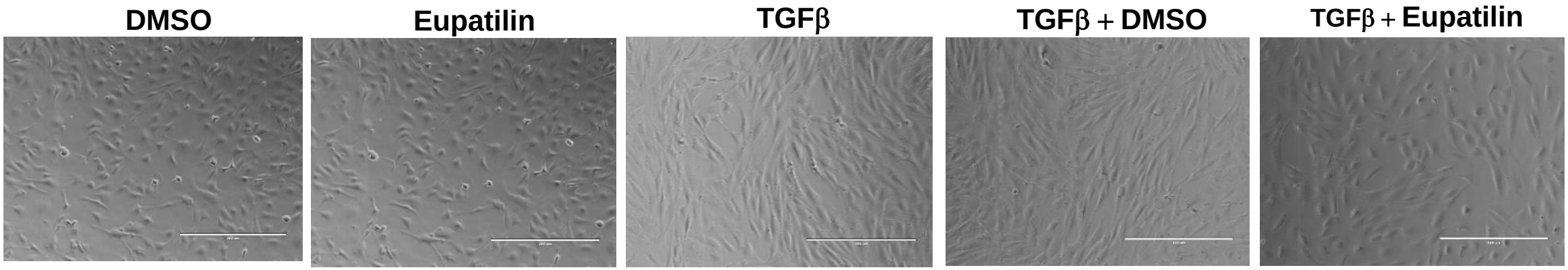
DMSO
Eupatilin
TGFβ
TGFβ + DMSO
TGFβ + Eupatilin

B)

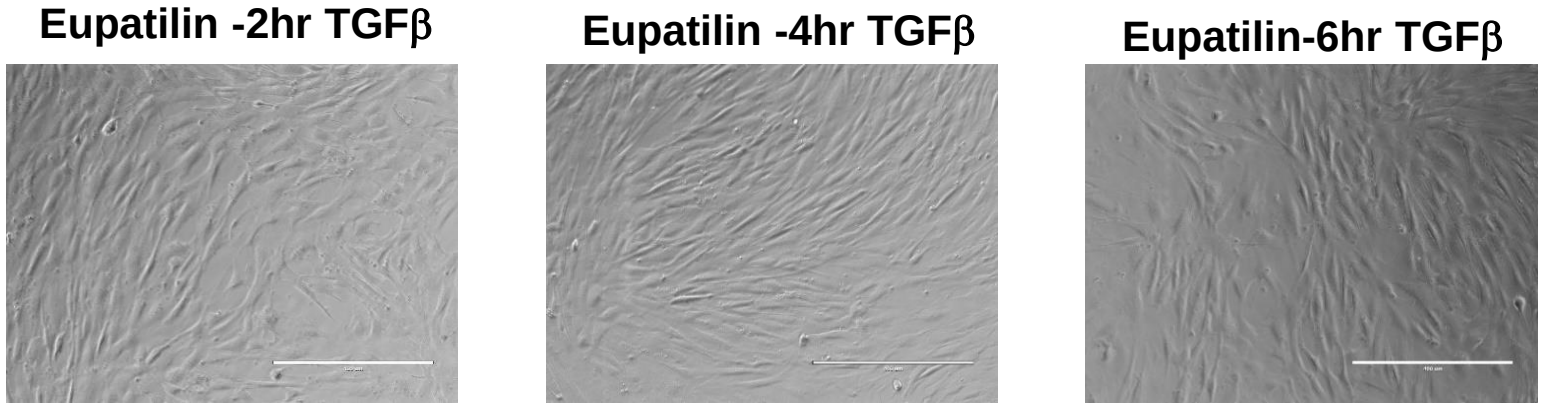
Eupatilin -2hr TGFβ
Eupatilin -4hr TGFβ
Eupatilin-6hr TGFβ

C)

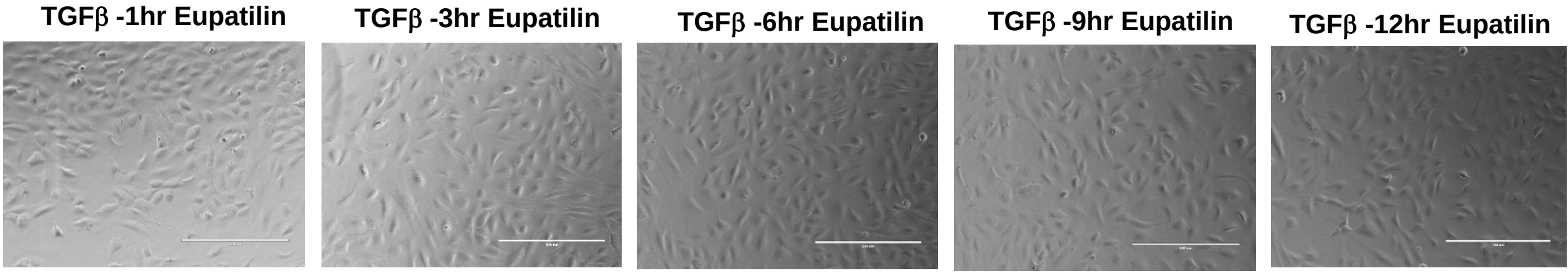
TGFβ -1hr Eupatilin
TGFβ -3hr Eupatilin
TGFβ -6hr Eupatilin
TGFβ -9hr Eupatilin
TGFβ -12hr Eupatilin

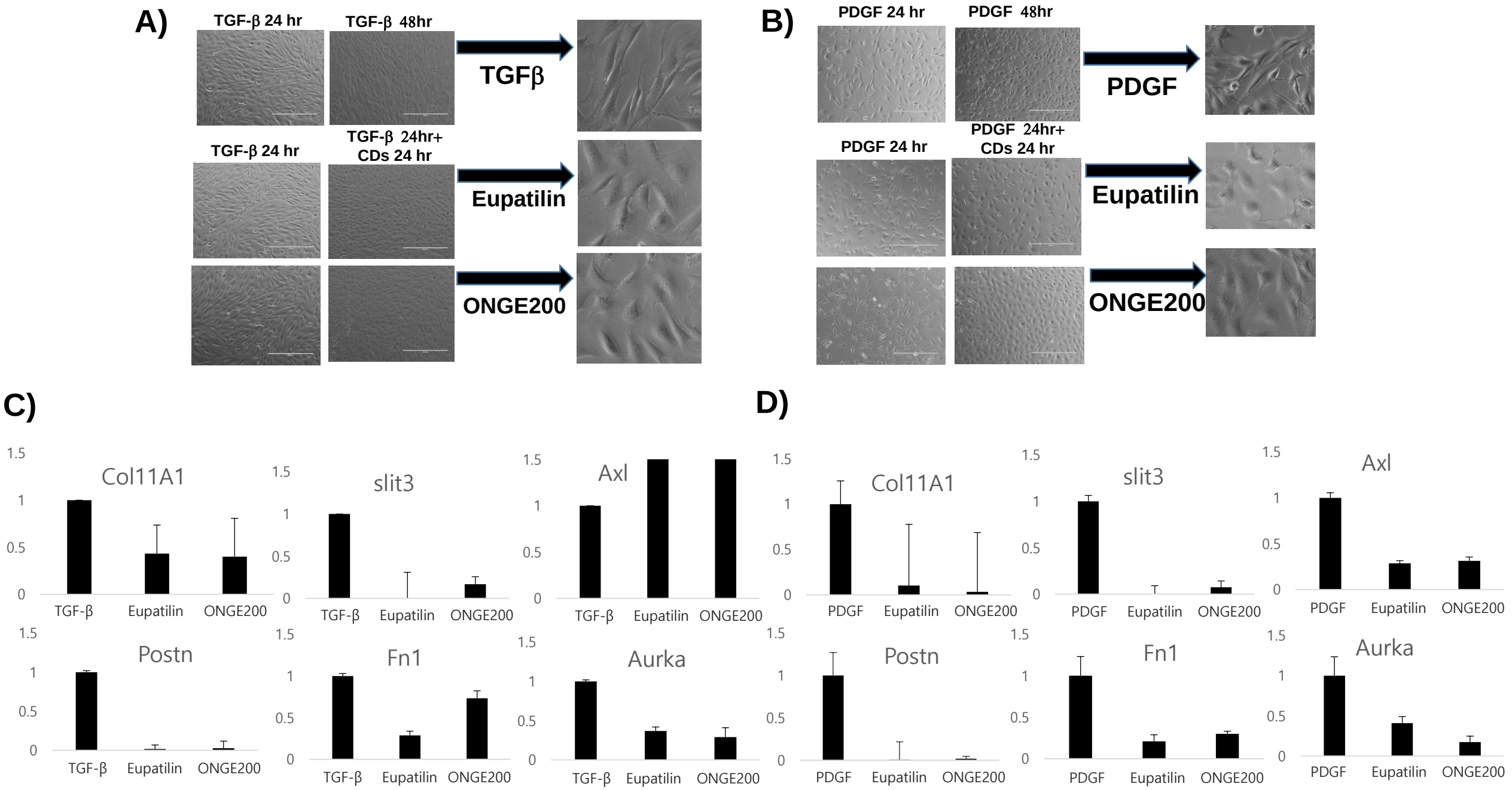
A)
TGF-β 24 hr
TGF-β 48hr
TGFβ
TGF-β 24 hr
TGF-β 24hr+ CDs 24 hr
Eupatilin
ONGE200
B)
PDGF 24 hr
PDGF 48hr
PDGF
PDGF 24 hr
PDGF 24hr+ CDs 24 hr
Eupatilin
ONGE200
C)
Col11A1
slit3
Axl
Postn
Fn1
Aurka
TGF-β
Eupatilin
ONGE200
D)
Col11A1
slit3
Axl
Postn
Fn1
Aurka
PDGF
Eupatilin
ONGE200

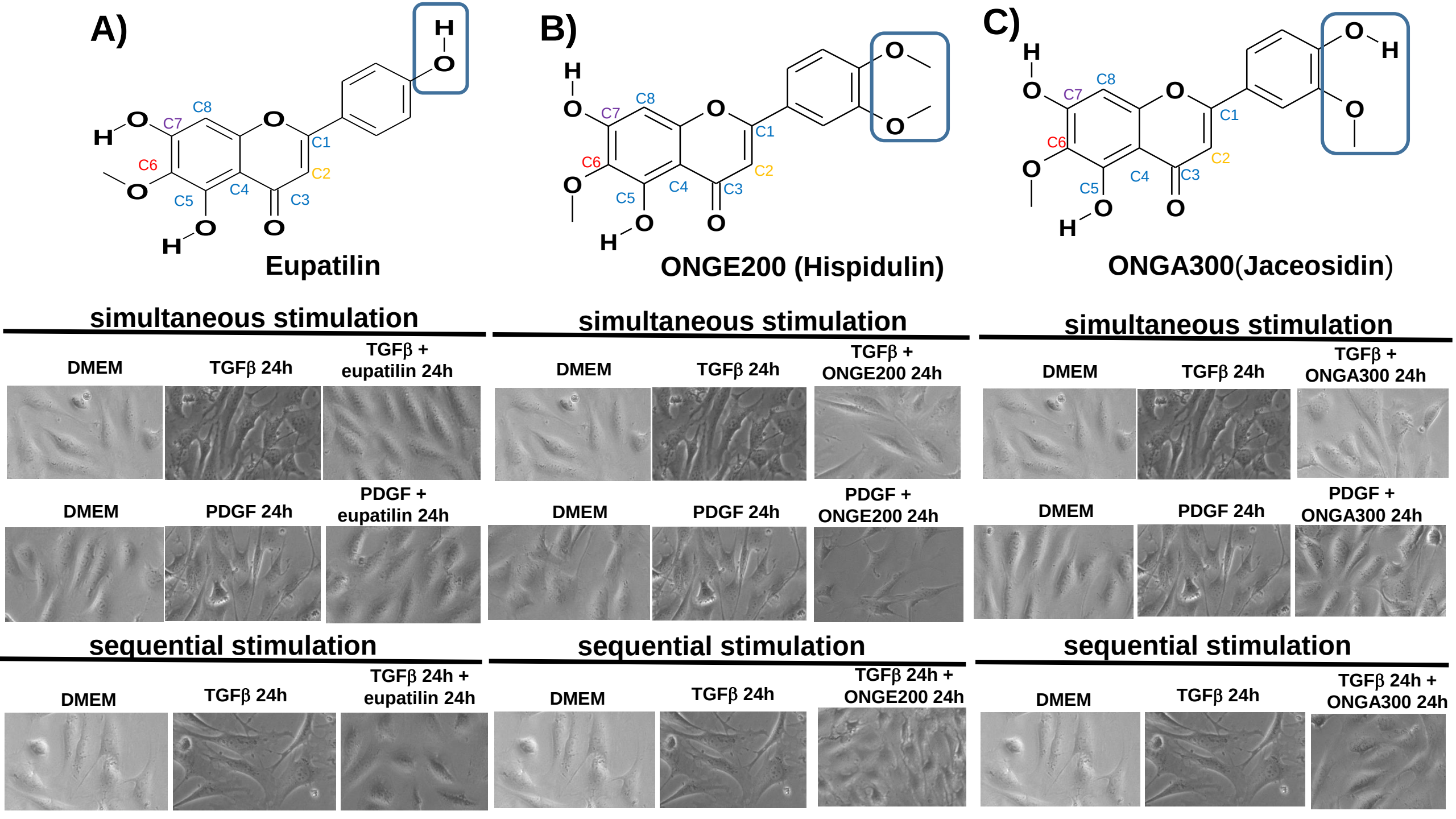
A)
Eupatilin
B)
ONGE200 (Hispidulin)
C)
ONGA300(Jaceosidin)
simultaneous stimulation
DMEM
TGFβ 24h
TGFβ + eupatilin 24h
DMEM
PDGF 24h
PDGF + eupatilin 24h
simultaneous stimulation
DMEM
TGFβ 24h
TGFβ + ONGE200 24h
DMEM
PDGF 24h
PDGF + ONGE200 24h
simultaneous stimulation
DMEM
TGFβ 24h
TGFβ + ONGA300 24h
DMEM
PDGF 24h
PDGF + ONGA300 24h
sequential stimulation
DMEM
TGFβ 24h
TGFβ 24h + eupatilin 24h
sequential stimulation
DMEM
TGFβ 24h
TGFβ 24h + ONGE200 24h
sequential stimulation
DMEM
TGFβ 24h
TGFβ 24h + ONGA300 24h

Reprogramming EMT by Eupatilin

TGFβ

TGFβ
Eupatilin

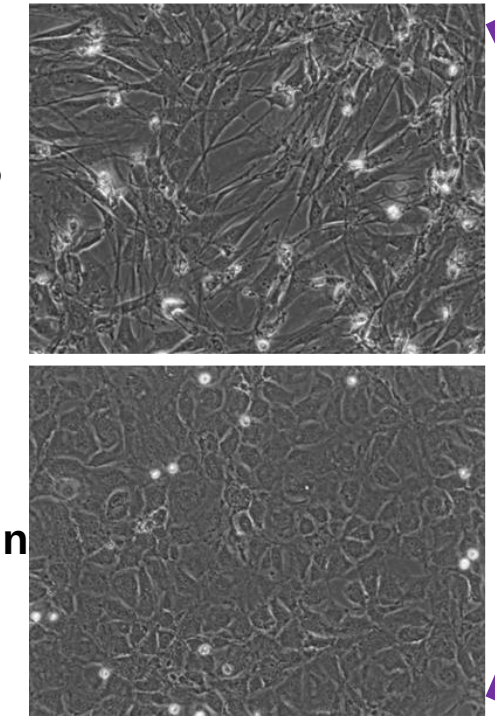

RNA-Seq

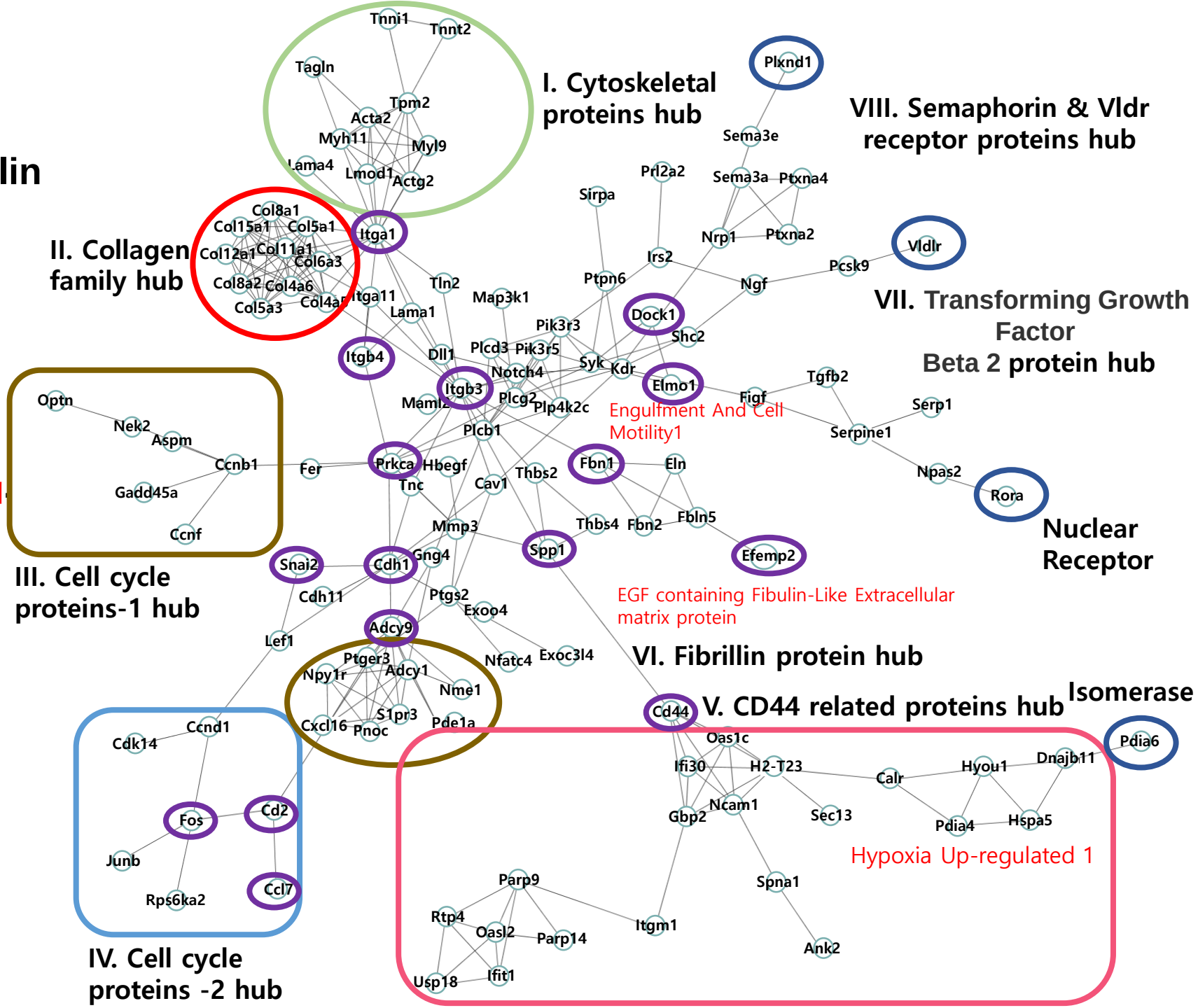

A)

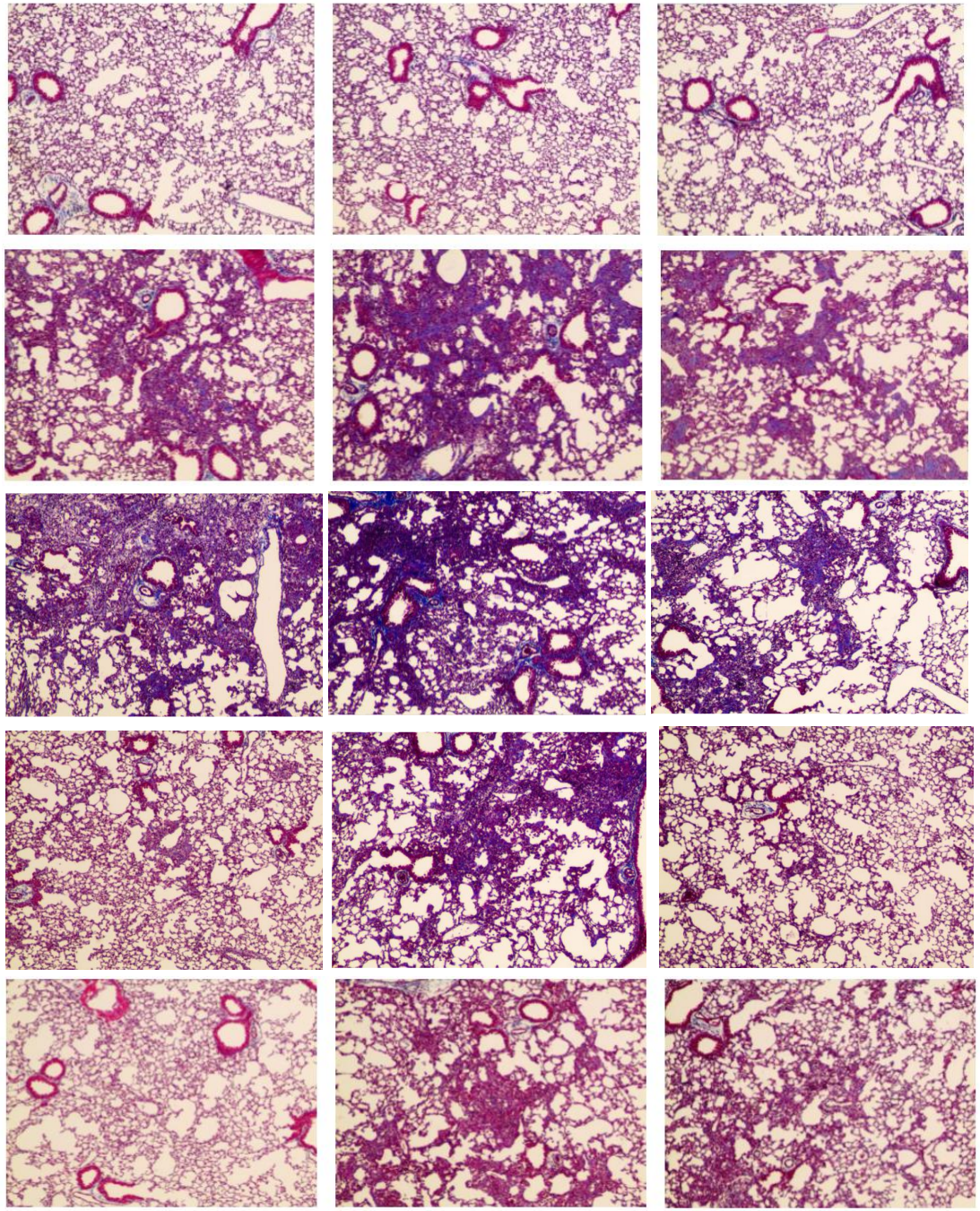

Vehicle control

Bleomycin

Bleomycin + Eupatilin (5μg)

Bleomycin + Eupatilin (20μg)

Bleomycin + Eupatilin (40μg)

B)

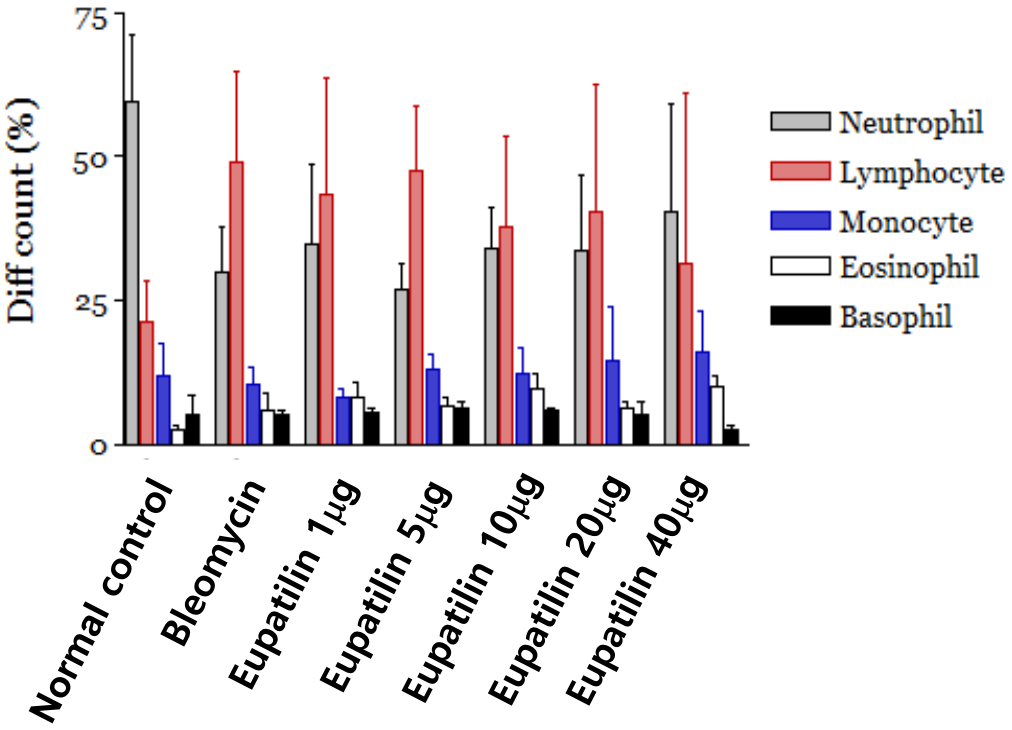

A)

No.	Description (Abbreviation)	Log2fc	p-value
1	Myosin IB (Myo1b)	-4.73	0.00005
2	Sphingosine kinase 1 (Sphk1)	-inf	0.00005
3	Myosin ID (Myo1d)	-6.27	0.00005
4	Jun dimerization protein 2 (Jdp2)	-4.23	0.00005
5	Scinderin (Scin)		0.00005
6	Matrix metallopeptidase 14		0.00005
7	Collagen Tripe helix repeat containing 1 (Cthrc1)	-inf	0.00005
8	Mesothelin (Msln)	-inf	0.00005
9	Desmoglein2 (Dsg2)	-inf	0.00005
10	Very Low Density Lipoprotein receptor (Vldlr)	-inf	no
11	Rous sarcoma oncogene (Src)	-5.04	0.00005
12	RAS guanyl releasing protein 1 (Rasgrp1)	-5.92	0.00005
13	Tropomyosin2 (Tpm2)	-inf	0.00005
14	Basic helix-loop-helix family, member e40 (Bhlhe40)	-3.25	0.00005
15	Integrin beta 3 (Itgb3)	-4.36	0.0001
16	Adhesin G protein-coupled receptor V1 (Adgrv1)	-inf	0.0001
17	Claudin 11 (Cldn11)	-inf	0.0001
18	Fos-like antigen2 (Fosl2)	-3.85	0.0002
19	PR domain containing 1, with ZNF domain (Prdm1)	-4.52	0.00025
20	Syndecan 1 (Sdc1)	-2.87	0.00035
21	Growth hormone receptor (Ghr)	-5.36	0.00035
22	Cadherin, EGF LAG seven-pass G-type receptor 1 (Celsr1)	-inf	0.00035
23	Spinster homolog 2 (Spns2)	-5.95	0.00045
24	CD74 antigen (invariant polypeptide of major histocompatibility comp les, class II antigen-associated, Cd74)	-3.71	0.00045

B)

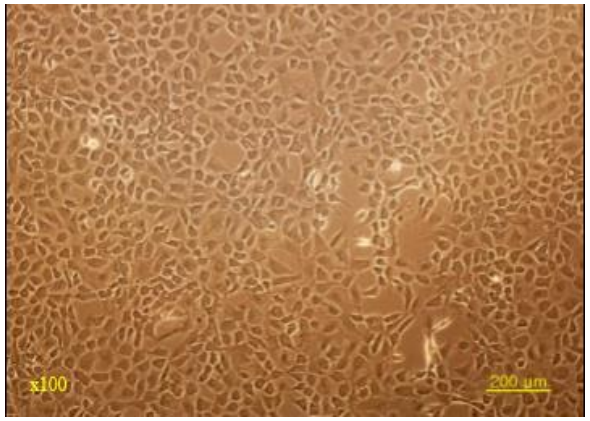

C)

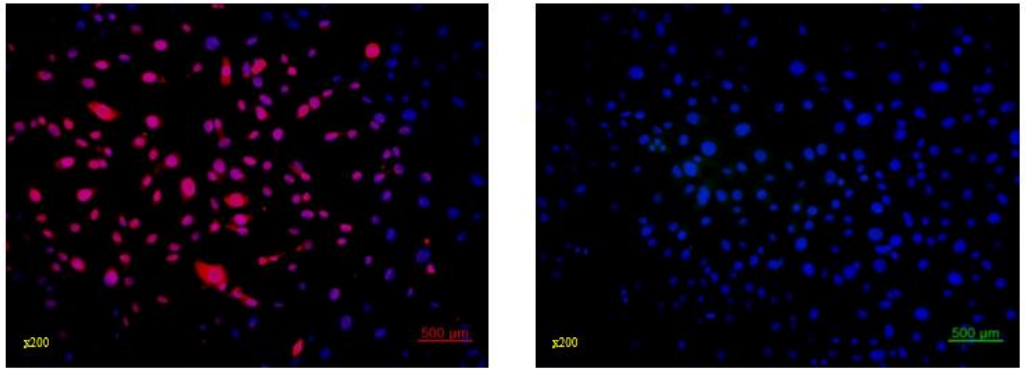

GATA4/DAPI

Cytokeratin18/DAPI

Supplementary Figure 1

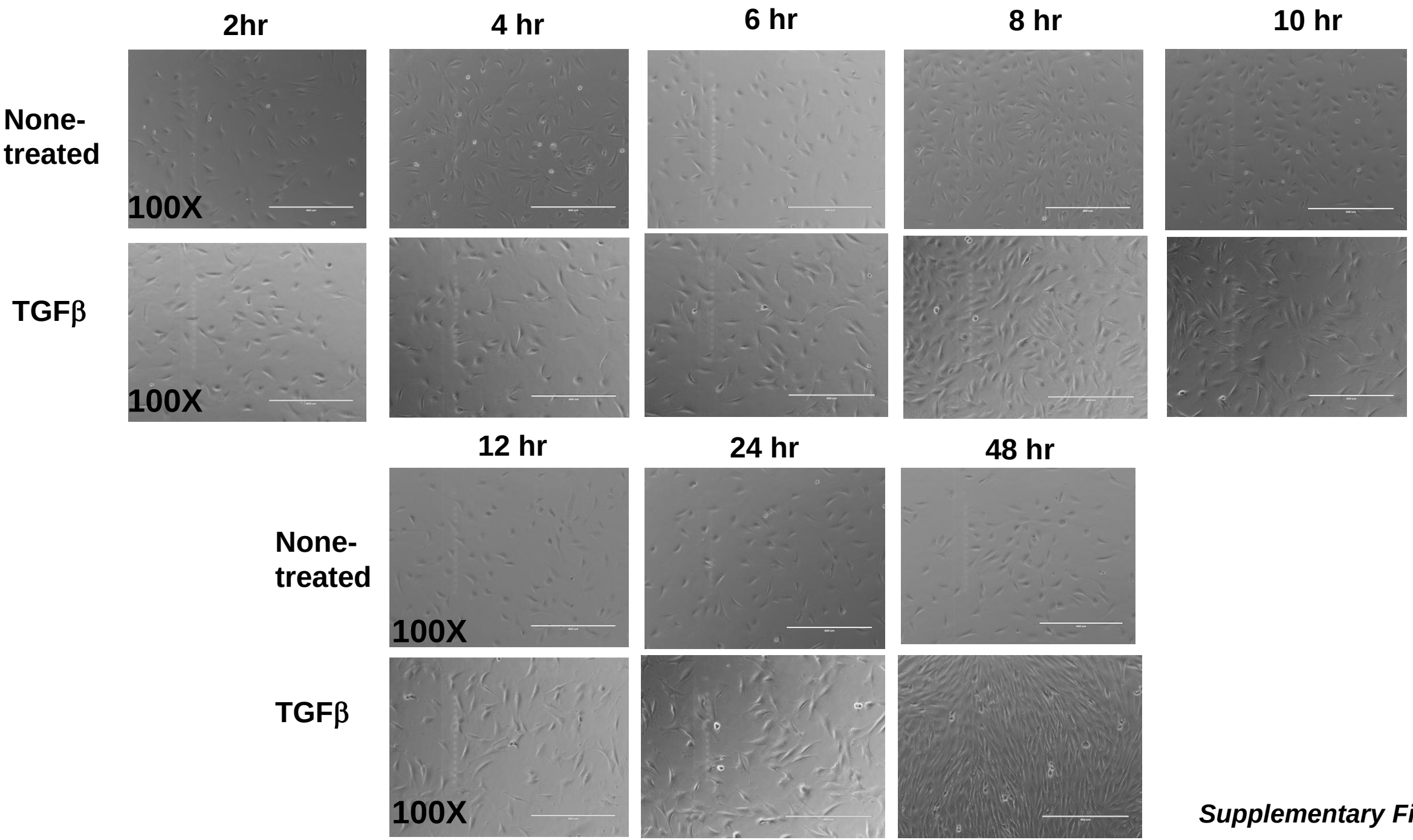

Supplementary Figure. 2

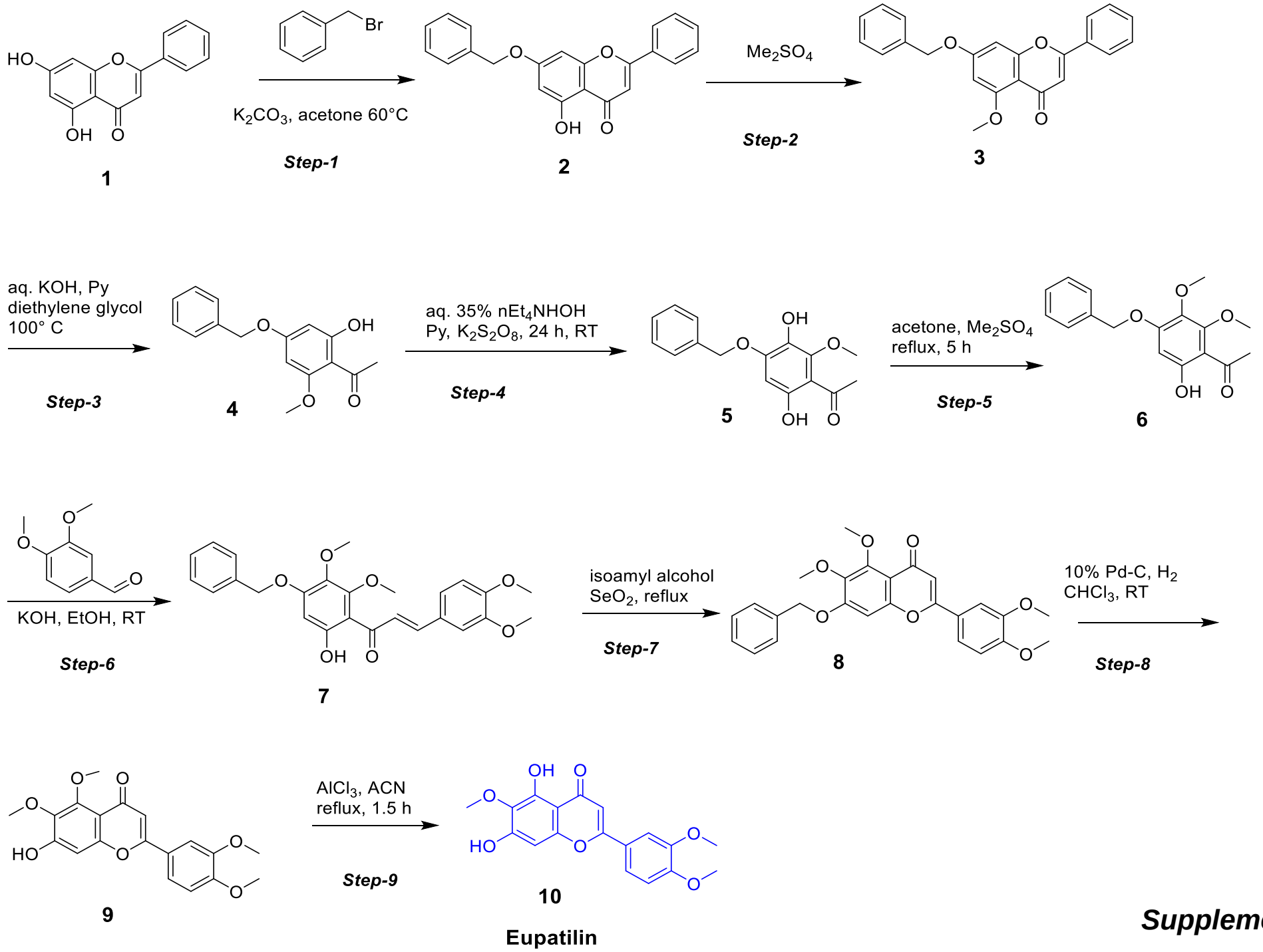

Supplementary Figure. 3

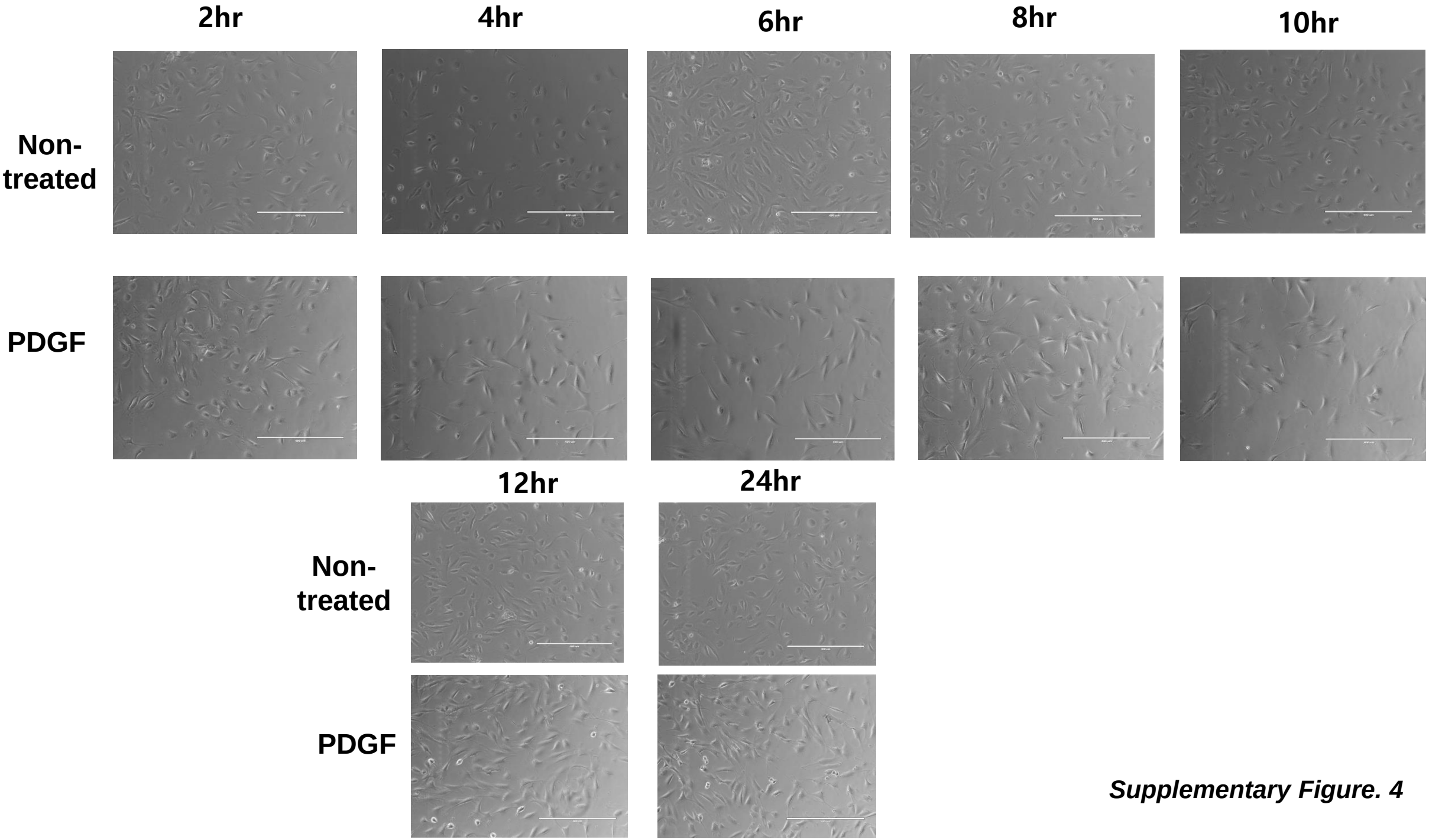

Supplementary Figure. 4

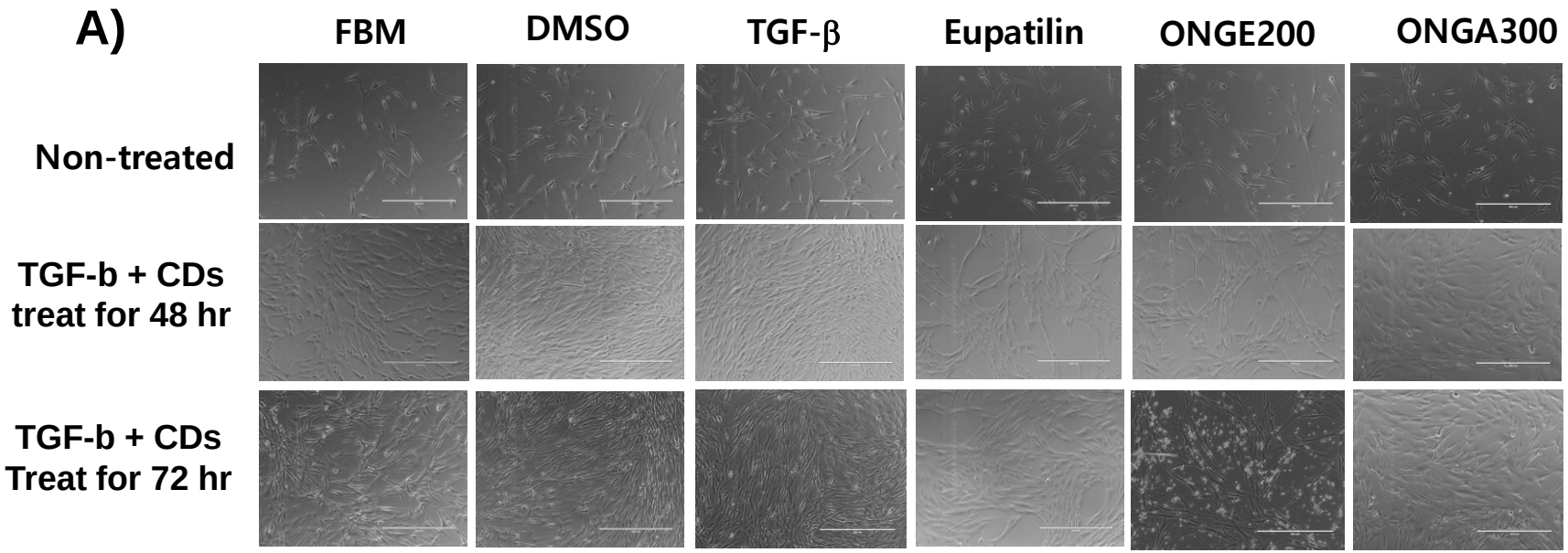

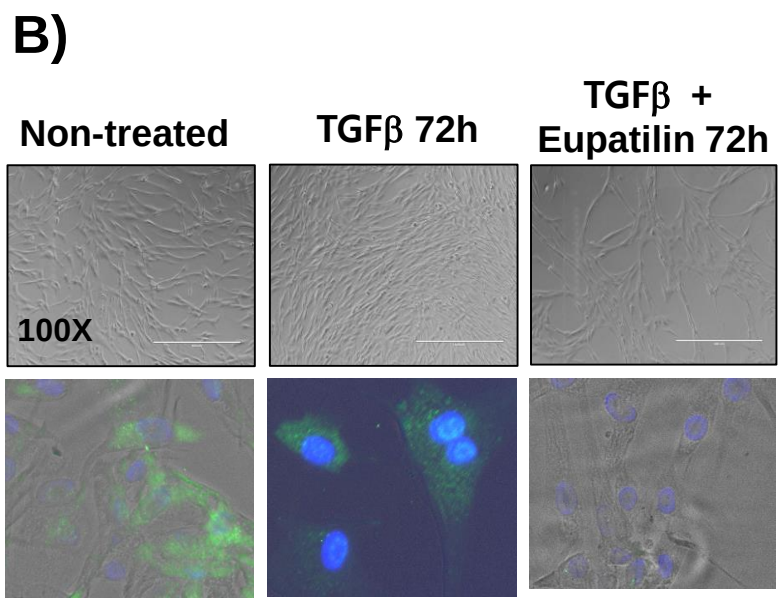

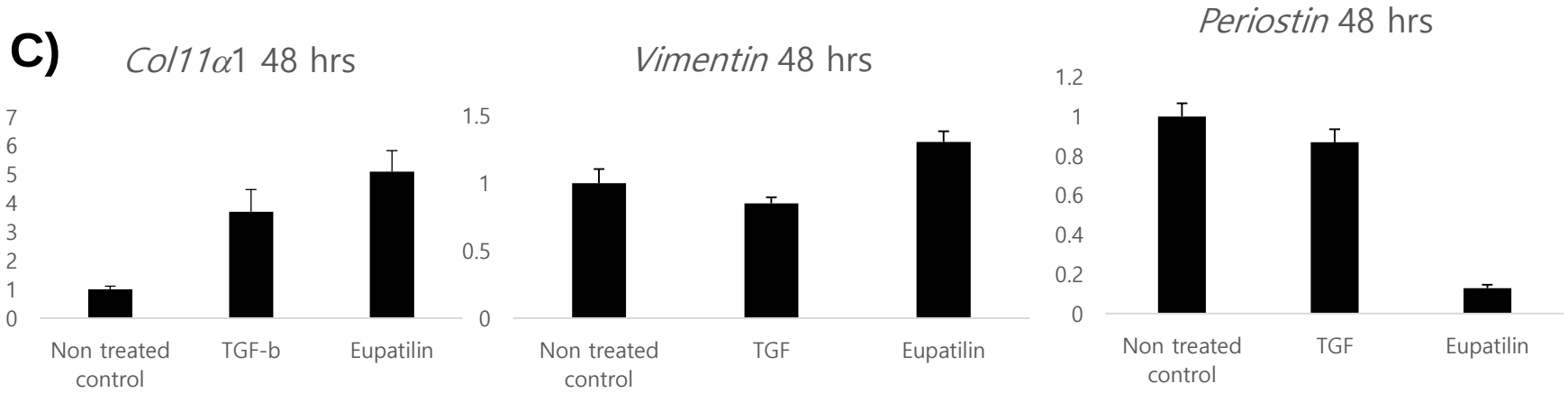

Supplementary Figure. 5

A) **TGFβ 24h**

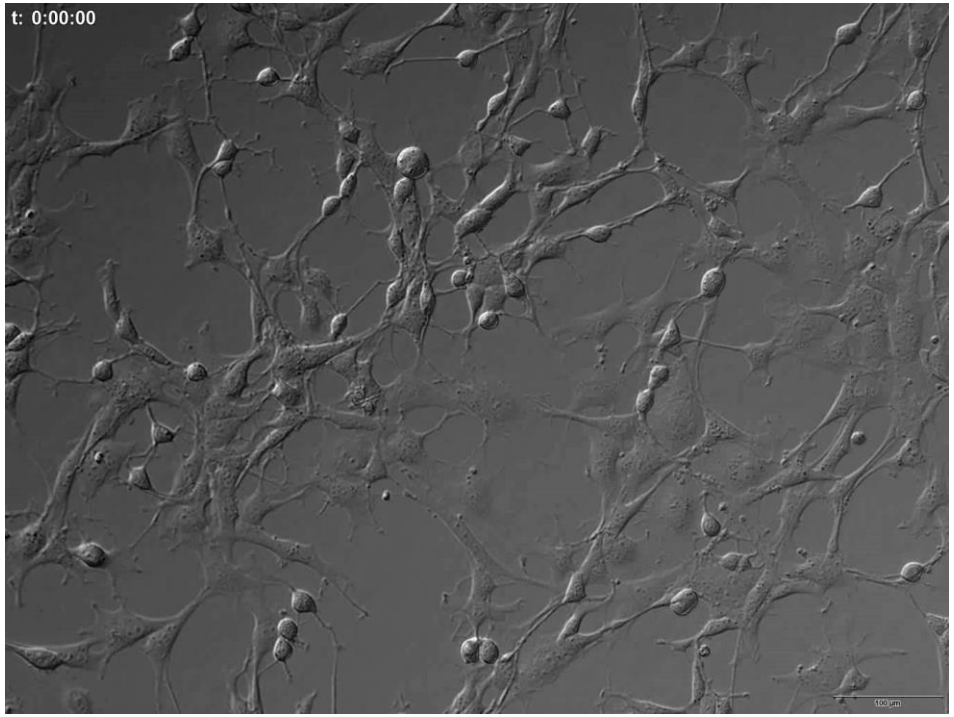

B) **(TGFβ + Eupatilin) 24h**

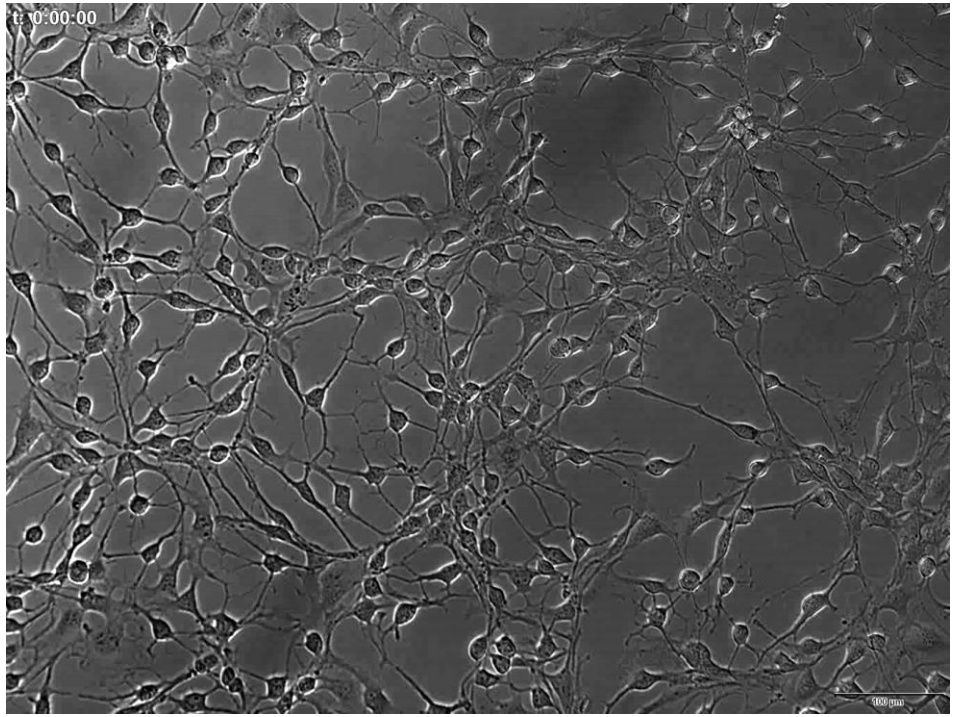

Supplementary Figure. 6

Group A

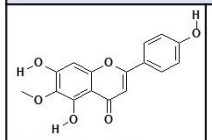 5,7-dihydroxy-2-(4-hydroxyphenyl)-6-methoxy-4H-chromen-4-one **(ONGE200)** **(Hispidulin)**	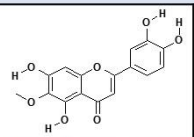 2-(3,4-dihydroxyphenyl)-5,7-dihydroxy-6-methoxy-4H-chromen-4-one (**ONGI300**)	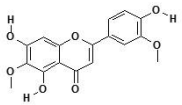 5,7-dihydroxy-2-(4-hydroxy-3-methoxyphenyl)-6-methoxy-4H-chromen - 4-one (**ONGA300**) (**Jaceosidin**)

Group B

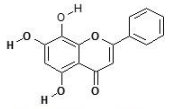 5,7,8-trihydroxy-2-phenyl-4H-chromen-4-one (**ONGG200**)	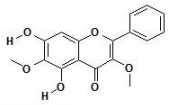 5,7-dihydroxy-3,6-dimethoxy-2-phenyl-4H-chromen-4-one (**ONGF300**)	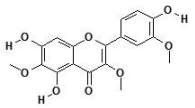 5,7-dihydroxy-2-(4-hydroxy-3-methoxyphenyl)-3,6-dimethoxy-4H-chromen-4-one (**ONGH300**)	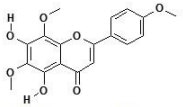 5,7-dihydroxy-6,8-dimethoxy-2-(4-methoxyphenyl)-4H-chromen-4-one (**ONGB400**)	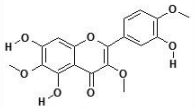 5,7-dihydroxy-2-(3-hydroxy-4-methoxyphenyl)-3,6-dimethoxy-4H-chromen-4-one (**ONGD400**)
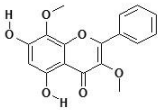 5,7-dihydroxy-3,8-dimethoxy-2-phenyl-4H-chromen-4-one (**ONGA100**)	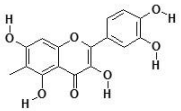 2-(3,4-dihydroxyphenyl)-3,5,7-trihydroxy-6-methyl-4H-chromen-4-one (**ONGG100**) (**Quercetin-like**)	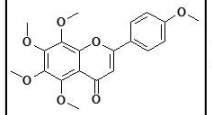 5,6,7,8-tetramethoxy-2-(4-methoxyphenyl)-4H-chromen-4-one (**ONGC300**)	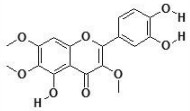 2-(3,4-dihydroxyphenyl)-5-hydroxy-3,6,7-trimethoxy-4H-chromen-4-one (**ONGG300**)	

Group C

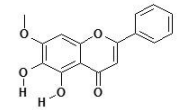 5,6-dihydroxy-7-methoxy-2-phenyl-4H-chromen-4-one (**ONGH100**)	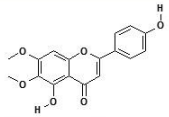 5-hydroxy-2-(4-hydroxyphenyl)-6,7-dimethoxy-4H-chromen-4-one (**ONGC200**)	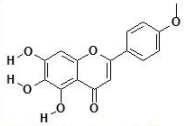 5,6,7-trihydroxy-2-(4-methoxyphenyl)-4H-chromen-4-one (**ONGD200**)
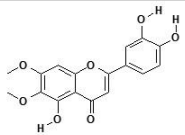 2-(3,4-dihydroxyphenyl)-5-hydroxy-6,7-dimethoxy -4H-chromen-4-one (**ONGH200**)	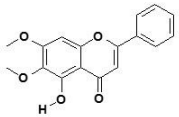 5-hydroxy-6,7-dimethoxy-2-phenyl-4H-chromen-4-one (**ONGE400**)	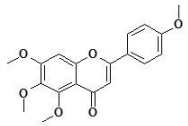 5,6,7-trimethoxy-2-(4-methoxyphenyl)-4H-chromen-4-one **(ONGG400)**

Group D

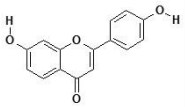 7-hydroxy-2-(4-hydroxyphenyl)-4H-chromen-4-one (**ONGC100**)	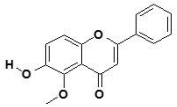 6-hydroxy-5-methoxy-2-phenyl-4H-chromen-4-one (**ONGE100**)	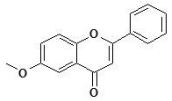 6-methoxy-2-phenyl-4H-chromen-4-one (**ONGF200**)	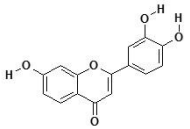 2-(3,4-dihydroxyphenyl)-7-hydroxy-4H-chromen-4-one (**ONGB300**) (**Luteolin-like**)	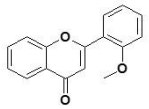 2-(2-methoxyphenyl)-4H-chromen-4-one (**ONGD300**)
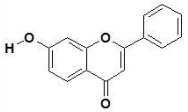 7-hydroxy-2-phenyl-4H-chromen-4-one (**ONGA400**)	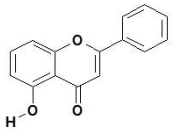 5-hydroxy-2-phenyl-4H-chromen-4-one (**ONGF400**)	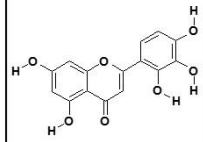 5,7-dihydroxy-2-(2,3,4-trihydroxyphenyl)-4H-chromen-4-one (**ONGE300**)	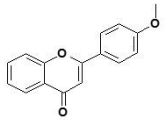 2-(4-methoxyphenyl)-4H-chromen-4-one (**ONGH400**)	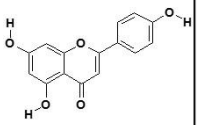 5,7-dihydroxy-2-(4-hydroxyphenyl)-4H-chromen-4-one (**Apigenin**)

Group E

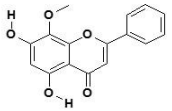 5,7-dihydroxy-8-methoxy-2-phenyl-4H-chromen-4-one (**ONGB100**)(**Wogonin**)	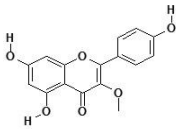 5,7-dihydroxy-2-(4-hydroxyphenyl)-3-methoxy-4H-chromen-4-one (**ONGB200**)	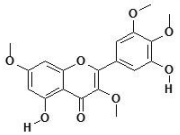 5-hydroxy-2-(3-hydroxy-4,5-dimethoxyphenyl)-3,7-dimethoxy-4H-chromen-4-one (**ONGA200**)
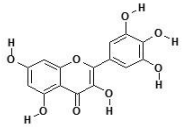 3,5,7-trihydroxy-2-(3,4,5-trihydroxyphenyl)-4H-chromen-4-one (**ONGD100**)(**Myricetin**)	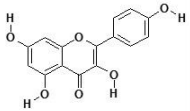 3,5,7-trihydroxy-2-(4-hydroxyphenyl)-4H-chromen-4-one (**ONGF100**)	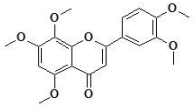 2-(3,4-dimethoxyphenyl)-5,7,8-trimethoxy-4H-chromen-4-one (**ONGC400**)

Supplementary Figure. 7

Simultaneous stimulation with TGFβ and CD members 24hrs

Name	Structure	TGF treat 전	TGF treat 24 hr
2-(3,4-dimethoxyphenyl)-5,7-dihydroxy-6-methoxy-4H-chromen-4-one (**ONG2**)(**Eupatilin**)	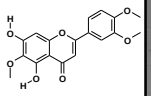	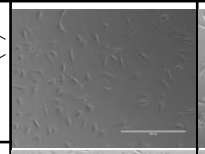	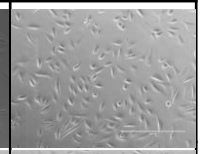
5,7-dihydroxy-3,8-dimethoxy-2-phenyl-4H-chromen-4-one (**ONGA100**)	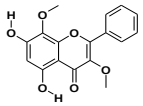		
5,7-dihydroxy-8-methoxy-2-phenyl-4H-chromen-4-one (**ONGB100**)(**Wogonin**)	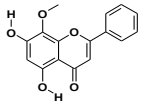	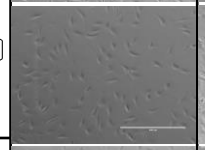	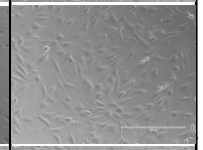
7-hydroxy-2-(4-hydroxyphenyl)-4H-chromen-4-one (**ONGC100**)	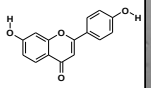	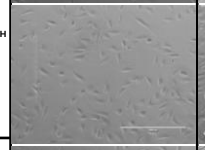	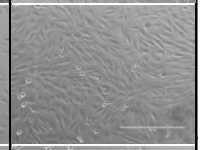
3,5,7-trihydroxy-2-(3,4,5-trihydroxyphenyl)-4H-chromen-4-one (**ONGD100**)(**Myricetin**)	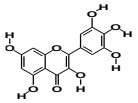		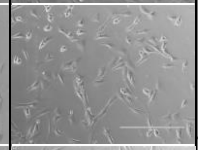
6-hydroxy-5-methoxy-2-phenyl-4H-chromen-4-one (**ONGE100**)	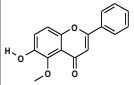	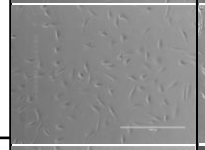	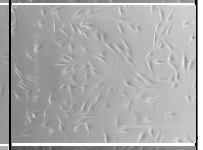
3,5,7-trihydroxy-2-(4-hydroxyphenyl)-4H-chromen-4-one (**ONGF100**)	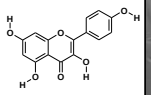		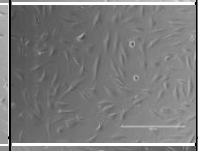
2-(3,4-dihydroxyphenyl)-3,5,7-trihydroxy-6-methyl-4H-chromen-4-one (**ONGG100**)(**Quercetin-like**)	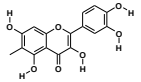		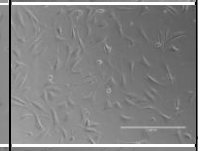
5,6-dihydroxy-7-methoxy-2-phenyl-4H-chromen-4-one (**ONGH100**)	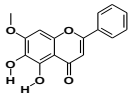	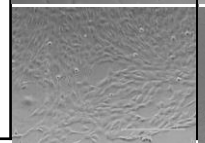	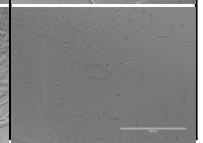

Name	Structure	TGF treat 전	TGF treat 24 hr
5-hydroxy-2-(3-hydroxy-4,5-dimethoxyphenyl)-3,7-dimethoxy-4H-chromen-4-one (**ONGA200**)	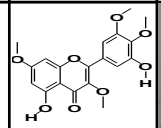	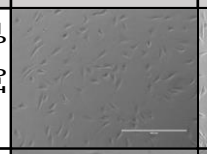	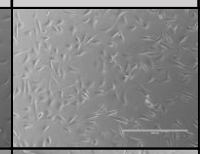
5,7-dihydroxy-2-(4-hydroxyphenyl)-3-methoxy-4H-chromen-4-one (**ONGB200**)	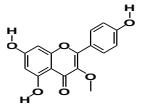	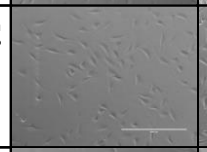	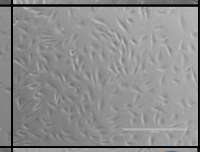
5-hydroxy-2-(4-hydroxyphenyl)-6,7-dimethoxy-4H-chromen-4-one (**ONGC200**)	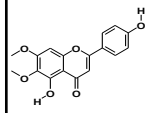	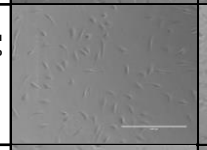	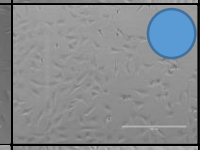
5,6,7-trihydroxy-2-(4-methoxyphenyl)-4H-chromen-4-one (**ONGD200**)	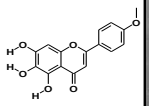	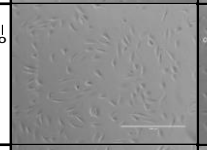	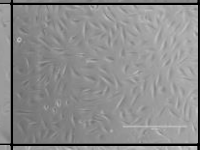
5,7-dihydroxy-2-(4-hydroxyphenyl)-6-methoxy-4H-chromen-4-one **(ONGE200) (Hispidulin)**	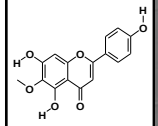	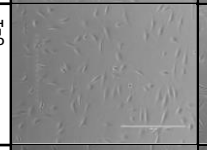	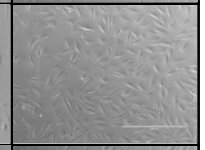
6-methoxy-2-phenyl-4H-chromen-4-one (**ONGF200**)	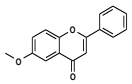	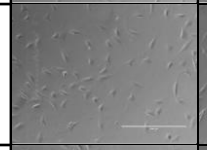	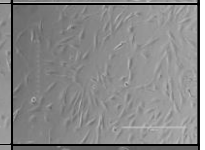
5,7,8-trihydroxy-2-phenyl-4H-chromen-4-one (**ONGG200**)	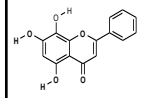	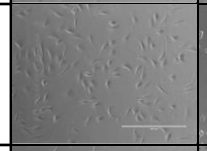	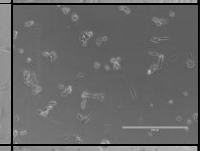
2-(3,4-dihydroxyphenyl)-5-hydroxy-6,7-dimethoxy-4H-chromen-4-one (**ONGH200**)	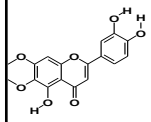	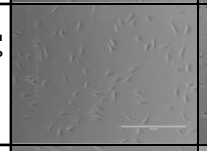	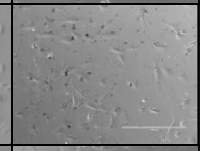
5,7-dihydroxy-2-(4-hydroxy-3-methoxyphenyl)-6-methoxy-4H-chromen-4-one (**ONGA300**)(**Jaceosidin**)	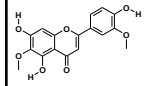	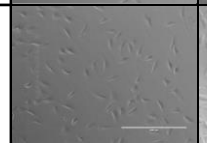	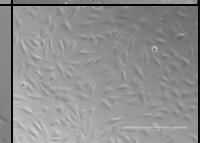

Supplementary Figure. 8-1

Simultaneous stimulation with TGFβ and CD members 24hrs

Name	Structure	TGF treat 전	TGF treat 24 hr
2-(3,4-dihydroxyphenyl)-5,7-dihydroxy-6-methoxy-4H-chromen-4-one (**ONGI300**)	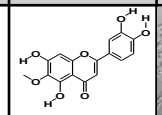	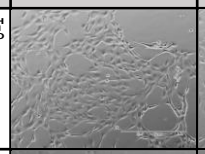	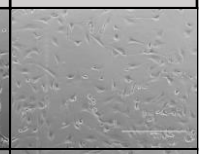
2-(3,4-dihydroxyphenyl)-7-hydroxy-4H-chromen-4-one (**ONGB300**)(**Luteolin-like**)	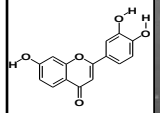	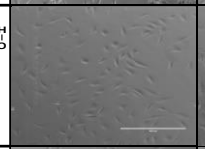	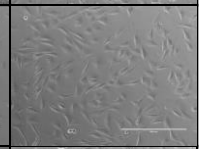
5,6,7,8-tetramethoxy-2-(4-methoxyphenyl)-4H-chromen-4-one (**ONGC300**)	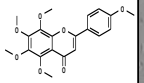	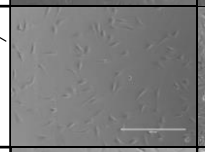	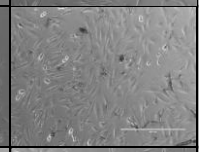
2-(2-methoxyphenyl)-4H-chromen-4-one (**ONGD300**)	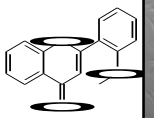	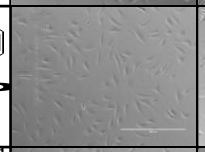	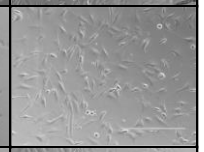
5,7-dihydroxy-2-(2,3,4-trihydroxyphenyl)-4H-chromen-4-one (**ONGE300**)	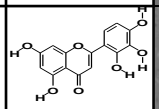	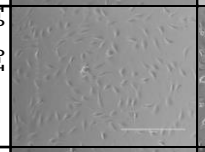	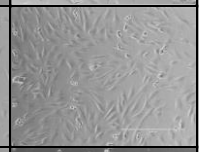
5,7-dihydroxy-3,6-dimethoxy-2-phenyl-4H-chromen-4-one (**ONGF300**)	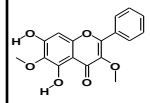	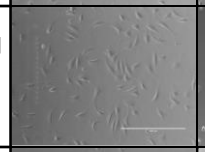	
2-(3,4-dihydroxyphenyl)-5-hydroxy-3,6,7-trimethoxy-4H-chromen-4-one (**ONGG300**)	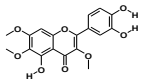	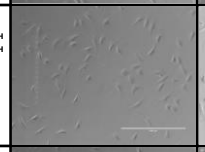	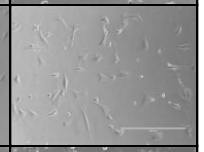
5,7-dihydroxy-2-(4-hydroxy-3-methoxyphenyl)-3,6-dimethoxy-4H-chromen-4-one (**ONGH300**)	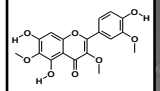	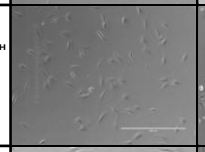	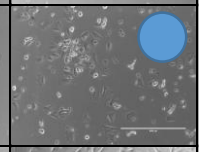
DMEM only		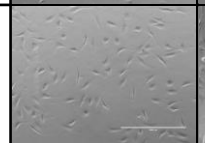	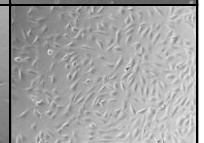

Name	Structure	TGF treat 전	TGF treat 24 hr
7-hydroxy-2-phenyl-4H-chromen-4-one (**ONGA400**)	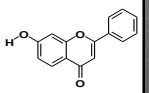	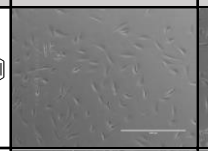	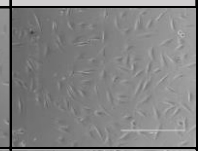
5,7-dihydroxy-6,8-dimethoxy-2-(4-methoxyphenyl)-4H-chromen-4-one (**ONGB400**)	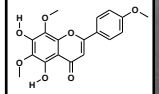	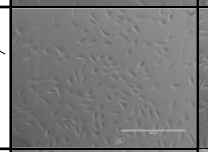	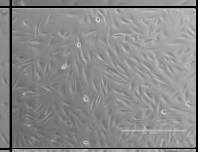
2-(3,4-dimethoxyphenyl)-5,7,8-trimethoxy-4H-chromen-4-one (**ONGC400**)	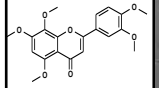	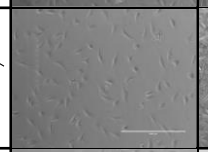	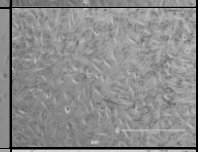
5,7-dihydroxy-2-(3-hydroxy-4-methoxyphenyl)-3,6-dimethoxy-4H-chromen-4-one (**ONGD400**)	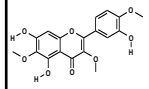	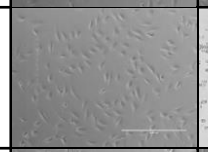	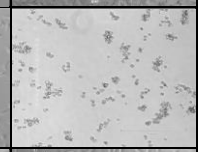
5-hydroxy-6,7-dimethoxy-2-phenyl-4H-chromen-4-one (**ONGE400**)	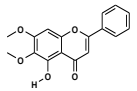	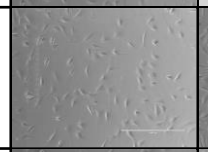	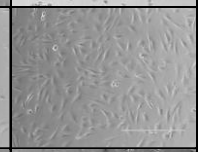
5-hydroxy-2-phenyl-4H-chromen-4-one (**ONGF400**)	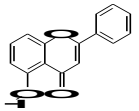	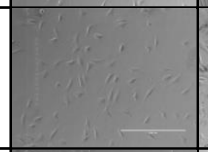	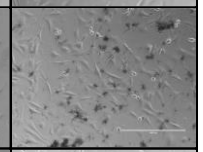
5,6,7-trimethoxy-2-(4-methoxyphenyl)-4H-chromen-4-one (**ONGG400**)	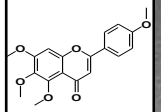	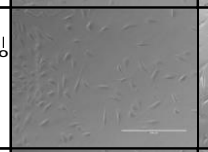	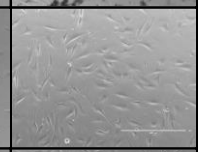
2-(4-methoxyphenyl)-4H-chromen-4-one (**ONGH400**)	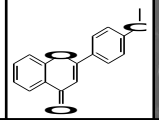	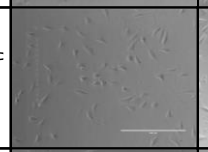	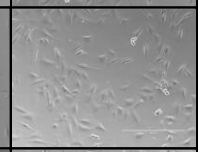
TGF-b only		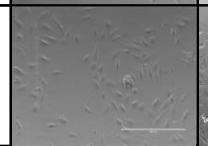	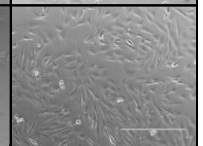

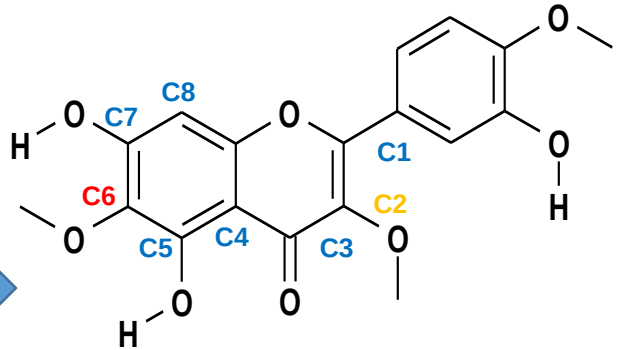

5,7-dihydroxy-2-(3-hydroxy-4-methoxyphenyl)-3,6-dimethoxy-4H-chromen-4-one (**ONGD400**)

Non-treated	TGF-β	50μM	25μM	10μM

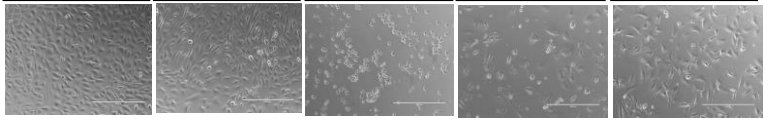

Supplementary Figure. 8-2

sequential stimulation with TGFβ and CD members

Name	Structure	TGF-b treat 전	TGF-b treat 24 hr	Analogue treat 24 hr
2-(3,4-dimethoxyphenyl)-5,7-dihydroxy-6-methoxy-4H-chromen-4-one (**ONG2**)(**Eupatilin**)	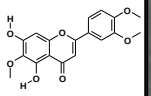	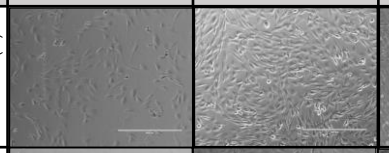	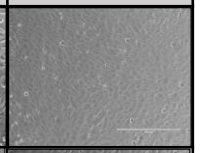	
5,7-dihydroxy-3,8-dimethoxy-2-phenyl-4H-chromen-4-one (**ONGA100**)	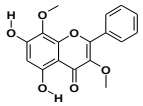	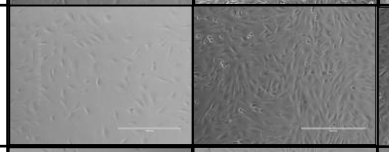	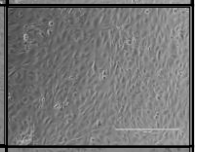	
5,7-dihydroxy-8-methoxy-2-phenyl-4H-chromen-4-one (**ONGB100**)(**Wogonin**)	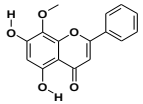	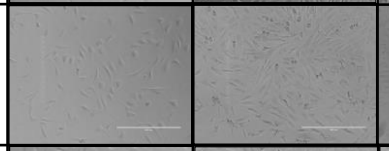	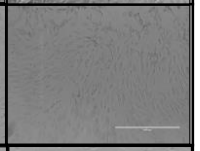	
7-hydroxy-2-(4-hydroxyphenyl)-4H-chromen-4-one (**ONGC100**)	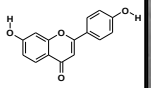	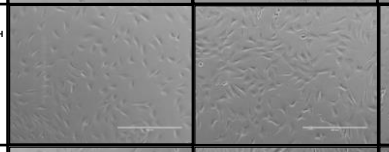	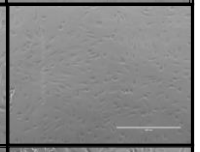	
3,5,7-trihydroxy-2-(3,4,5-trihydroxyphenyl)-4H-chromen-4-one (**ONGD100**)(**Myricetin**)	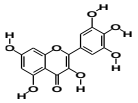	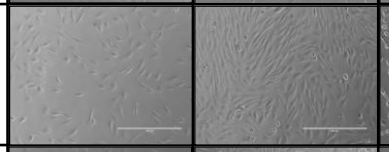	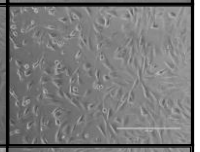	
6-hydroxy-5-methoxy-2-phenyl-4H-chromen-4-one (**ONGE100**)	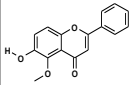	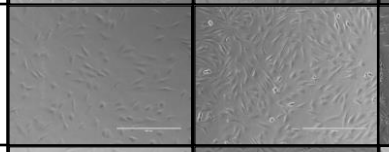	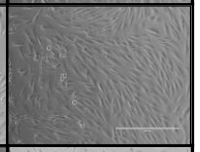	
3,5,7-trihydroxy-2-(4-hydroxyphenyl)-4H-chromen-4-one (**ONGF100**)	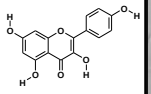	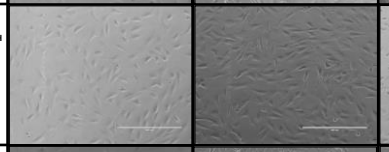	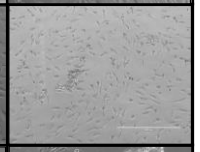	
2-(3,4-dihydroxyphenyl)-3,5,7-trihydroxy-6-methyl-4H-chromen-4-one (**ONGG100**)(**Quercetin-like**)	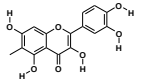	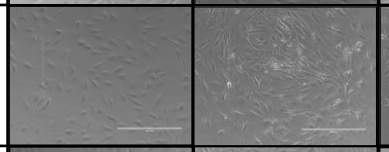	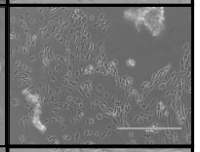	
5,6-dihydroxy-7-methoxy-2-phenyl-4H-chromen-4-one (**ONGH100**)	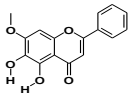	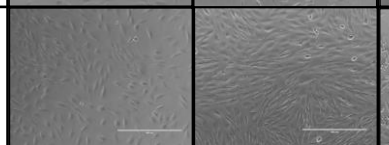	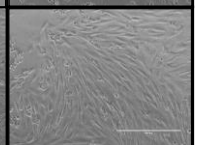	

Name	Structure	TGF-b treat 전	TGF-b treat 24 hr	Analogue treat 24 hr
5-hydroxy-2-(3-hydroxy-4,5-dimethoxyphenyl)-3,7-dimethoxy-4H-chromen-4-one (**ONGA200**)	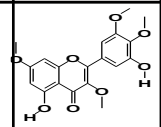	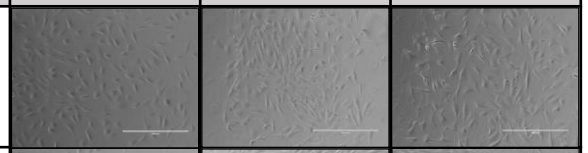		
5,7-dihydroxy-2-(4-hydroxyphenyl)-3-methoxy-4H-chromen-4-one (**ONGB200**)	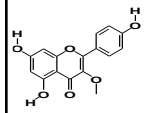	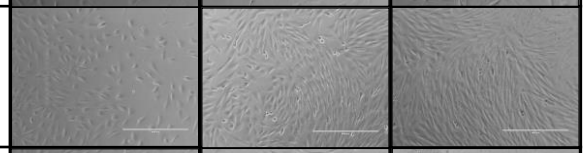		
5-hydroxy-2-(4-hydroxyphenyl)-6,7-dimethoxy-4H-chromen-4-one (**ONGC200**)	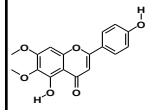	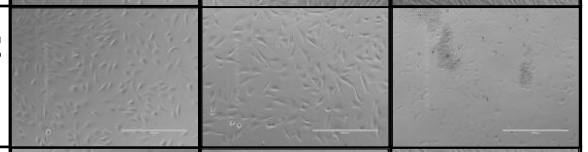		
5,6,7-trihydroxy-2-(4-methoxyphenyl)-4H-chromen-4-one (**ONGD200**)	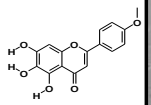	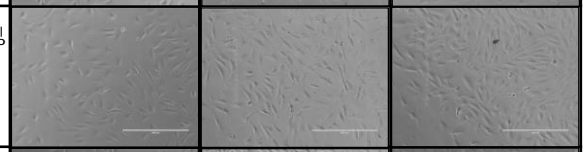		
5,7-dihydroxy-2-(4-hydroxyphenyl)-6-methoxy-4H-chromen-4-one **(ONGE200) (Hispidulin)**	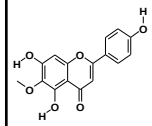	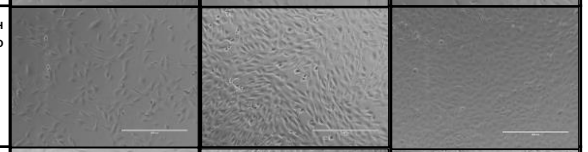		
6-methoxy-2-phenyl-4H-chromen-4-one (**ONGF200**)	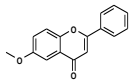	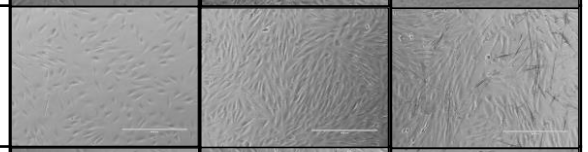		
5,7,8-trihydroxy-2-phenyl-4H-chromen-4-one (**ONGG200**)	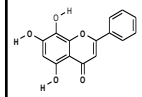	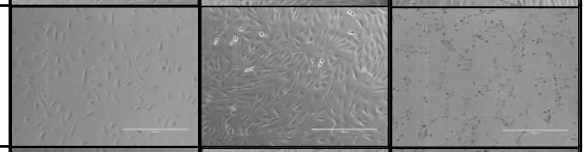		
2-(3,4-dihydroxyphenyl)-5-hydroxy-6,7-dimethoxy-4H-chromen-4-one (**ONGH200**)	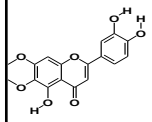	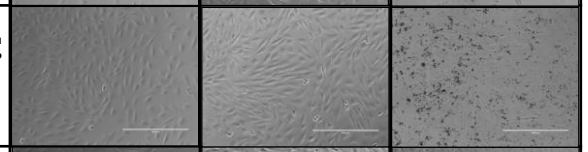		
5,7-dihydroxy-2-(4-hydroxy-3-methoxyphenyl)-6-methoxy-4H-chromen-4-one (**ONGA300**)(**Jaceosidin**)	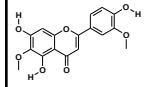	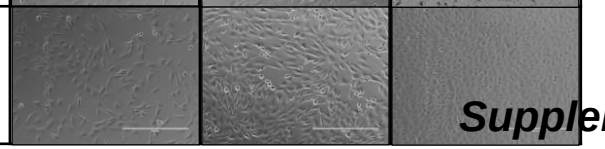		

Supplementary Figure. 9-1

sequential stimulation with TGFβ and CD members

Name	Structure	TGF-b treat 전	TGF-b treat 24 hr	Analogue treat 24 hr
2-(3,4-dihydroxyphenyl)-5,7-dihydroxy-6-methoxy-4H-chromen-4-one (**ONGI300**)	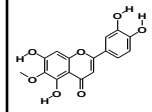	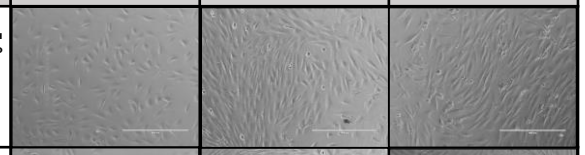		
2-(3,4-dihydroxyphenyl)-7-hydroxy-4H-chromen-4-one **(ONGB300)**(**Luteolin-like**)	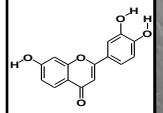	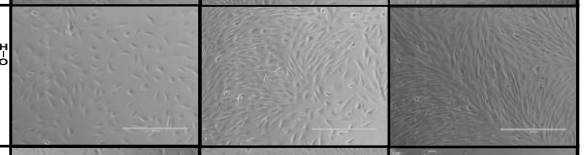		
5,6,7,8-tetramethoxy-2-(4-methoxyphenyl)-4H-chromen-4-one (**ONGC300**)	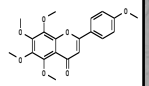	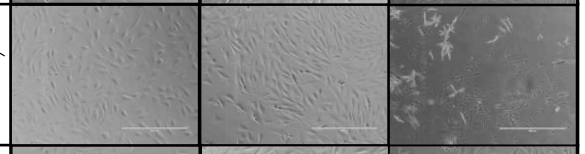		
2-(2-methoxyphenyl)-4H-chromen-4-one (**ONGD300**)	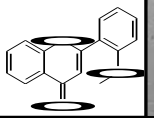	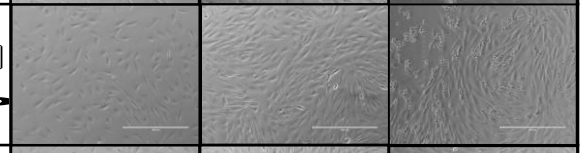		
5,7-dihydroxy-2-(2,3,4-trihydroxyphenyl)-4H-chromen-4-one (**ONGE300**)	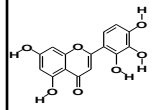	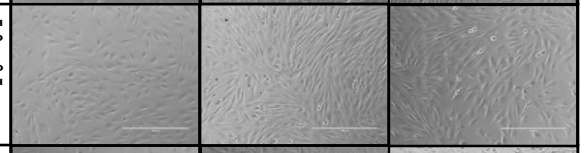		
5,7-dihydroxy-3,6-dimethoxy-2-phenyl-4H-chromen-4-one (**ONGF300**)	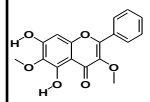	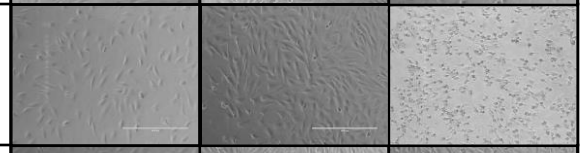		
2-(3,4-dihydroxyphenyl)-5-hydroxy-3,6,7-trimethoxy-4H-chromen-4-one (**ONGG300**)	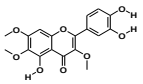	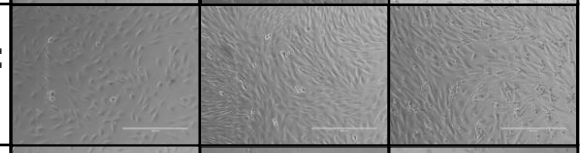		
5,7-dihydroxy-2-(4-hydroxy-3-methoxyphenyl)-3,6-dimethoxy-4H-chromen-4-one (**ONGH300**)	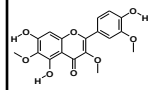	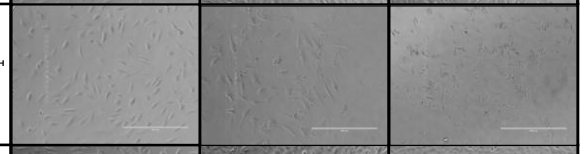		
DMEM only		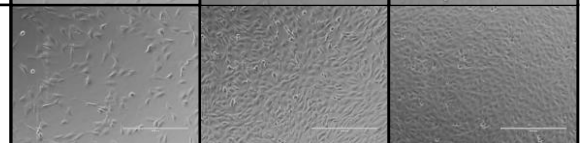		

Name	Structure	TGF-b treat 전	TGF-b treat 24 hr	Analogue treat 24 hr
7-hydroxy-2-phenyl-4H-chromen-4-one (**ONGA400**)	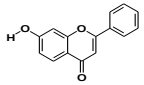	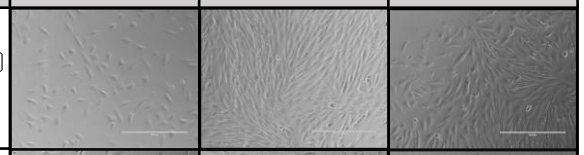		
5,7-dihydroxy-6,8-dimethoxy-2-(4-methoxyphenyl)-4H-chromen-4-one (**ONGB400**)	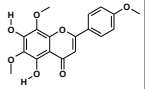	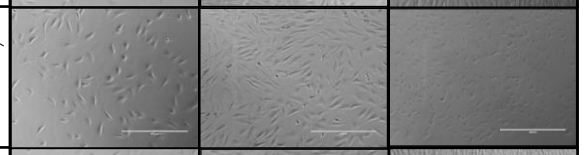		
2-(3,4-dimethoxyphenyl)-5,7,8-trimethoxy-4H-chromen-4-one (**ONGC400**)	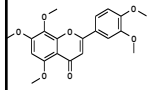	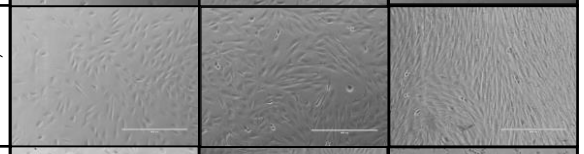		
5,7-dihydroxy-2-(3-hydroxy-4-methoxyphenyl)-3,6-dimethoxy-4H-chromen-4-one (**ONGD400**)	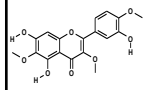	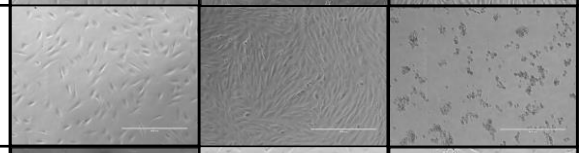		
5-hydroxy-6,7-dimethoxy-2-phenyl-4H-chromen-4-one (**ONGE400**)	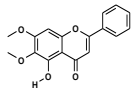	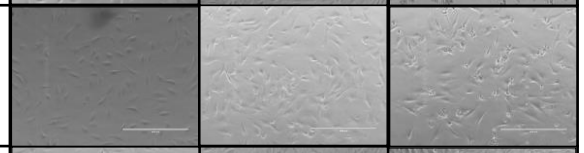		
5-hydroxy-2-phenyl-4H-chromen-4-one (**ONGF400**)	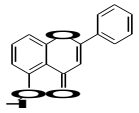	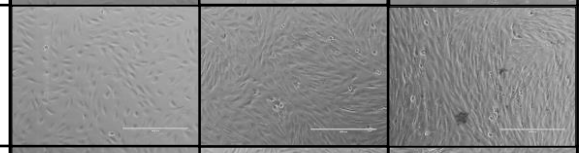		
5,6,7-trimethoxy-2-(4-methoxyphenyl)-4H-chromen-4-one **(ONGG400)**	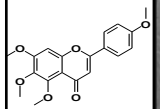	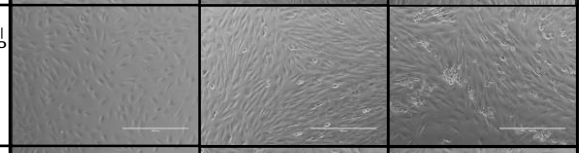		
2-(4-methoxyphenyl)-4H-chromen-4-one (**ONGH400)**	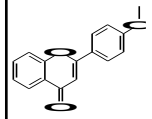	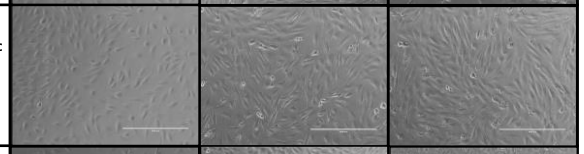		
TGF-b only		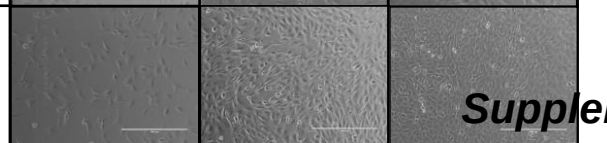		

Supplementary Figure. 9-2

sequential stimulation with PDGF and CD members

Name	Structure	PDGF treat 전	PDGF treat 24 hr	Analogue treat 24 hr
2-(3,4-dimethoxyphenyl)-5,7-dihydroxy-6-methoxy-4H-chromen-4-one (**ONG2**)(**Eupatilin**)	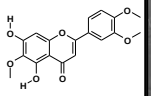	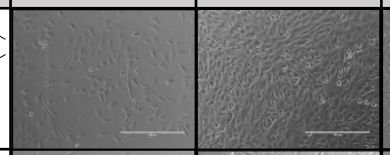	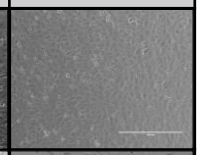	
5,7-dihydroxy-8-methoxy-2-phenyl-4H-chromen-4-one (**ONGB100**)(**Wogonin**)	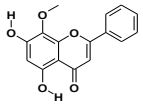	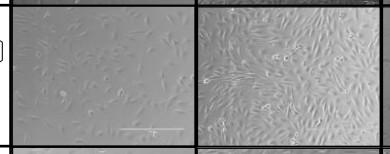	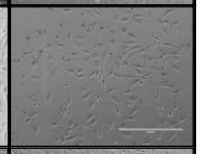	
7-hydroxy-2-(4-hydroxyphenyl)-4H-chromen-4-one (**ONGC100**)	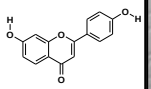	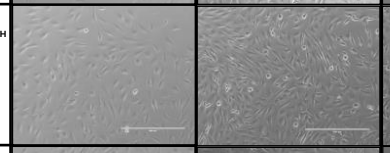	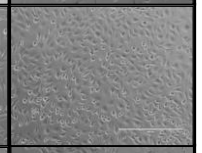	
3,5,7-trihydroxy-2-(3,4,5-trihydroxyphenyl)-4H-chromen-4-one (**ONGD100**)(**Myricetin**)	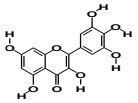	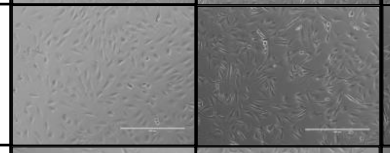	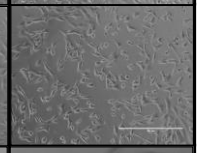	
6-hydroxy-5-methoxy-2-phenyl-4H-chromen-4-one (**ONGE100**)	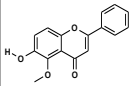	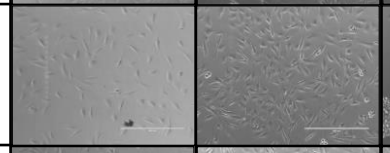	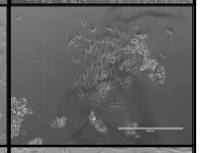	
3,5,7-trihydroxy-2-(4-hydroxyphenyl)-4H-chromen-4-one (**ONGF100**)	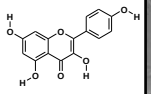	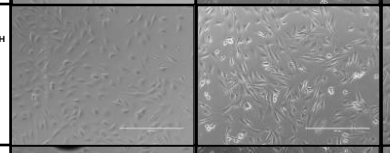	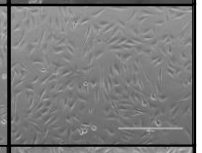	
2-(3,4-dihydroxyphenyl)-3,5,7-trihydroxy-6-methyl-4H-chromen-4-one (**ONGG100**)(**Quercetin-like**)	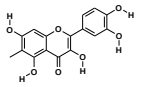	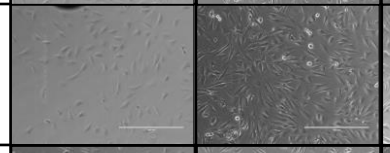	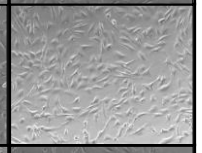	
5,6-dihydroxy-7-methoxy-2-phenyl-4H-chromen-4-one (**ONGH100**)	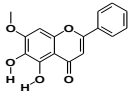	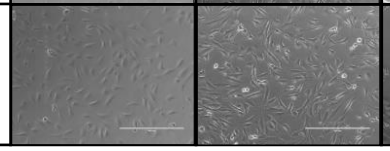	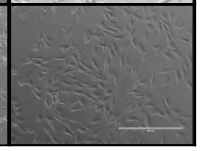	

Name	Structure	PDGF treat 전	PDGF treat 24 hr	Analogue treat 24 hr
5-hydroxy-2-(3-hydroxy-4,5-dimethoxyphenyl)-3,7-dimethoxy-4H-chromen-4-one (**ONGA200**)	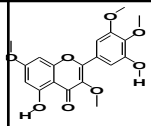	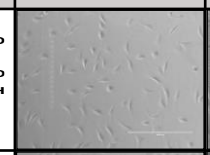	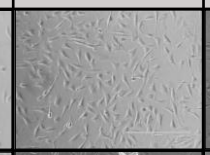	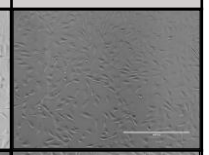
5,7-dihydroxy-2-(4-hydroxyphenyl)-3-methoxy-4H-chromen-4-one (**ONGB200**)	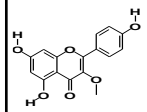	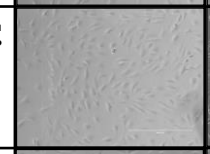	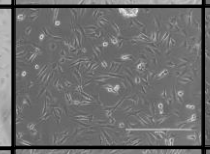	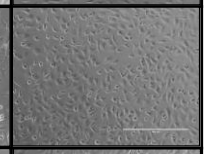
5-hydroxy-2-(4-hydroxyphenyl)-6,7-dimethoxy-4H-chromen-4-one (**ONGC200**)	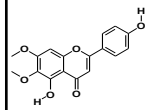	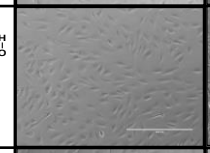	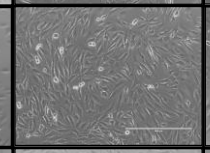	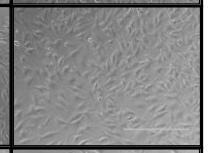
5,6,7-trihydroxy-2-(4-methoxyphenyl)-4H-chromen-4-one (**ONGD200**)	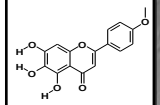	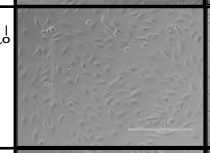	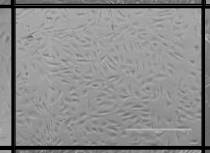	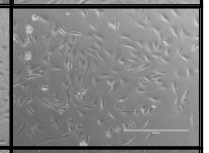
5,7-dihydroxy-2-(4-hydroxyphenyl)-6-methoxy-4H-chromen-4-one **(ONGE200) (Hispidulin)**	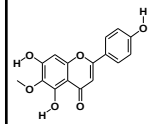	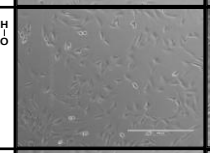	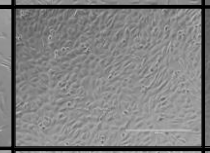	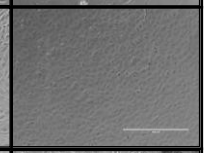
6-methoxy-2-phenyl-4H-chromen-4-one (**ONGF200**)	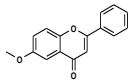	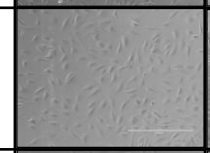	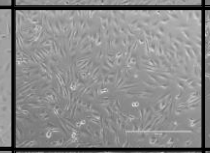	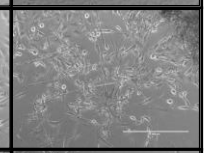
5,7,8-trihydroxy-2-phenyl-4H-chromen-4-one (**ONGG200**)	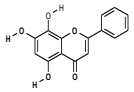	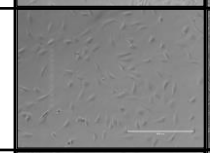	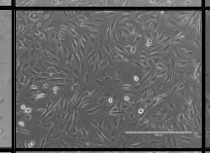	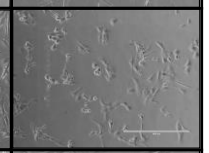
2-(3,4-dihydroxyphenyl)-5-hydroxy-6,7-dimethoxy-4H-chromen-4-one (**ONGH200**)	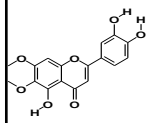	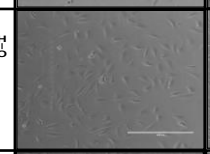	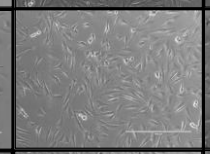	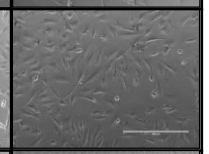
5,7-dihydroxy-2-(4-hydroxy-3-methoxyphenyl)-6-methoxy-4H-chromen-4-one (**ONGA300**)(**Jaceosidin**)	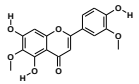	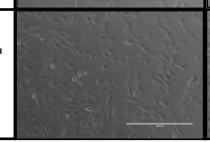	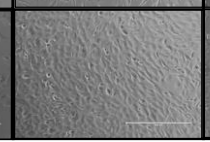	

Supplementary Figure. 10-1

sequential stimulation with PDGF and CD members

Name	Structure	PDGF treat 전	PDGF treat 24 hr	Analogue treat 24 hr
2-(3,4-dihydroxyphenyl)-5,7-dihydroxy-6-methoxy-4H-chromen-4-one (**ONGI300**)	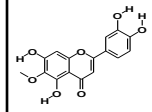	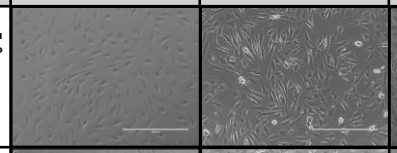	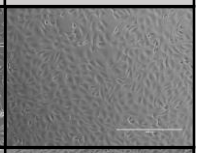	
2-(3,4-dihydroxyphenyl)-7-hydroxy-4H-chromen-4-one **(ONGB300)**(**Luteolin-like**)	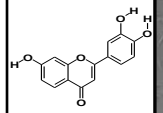	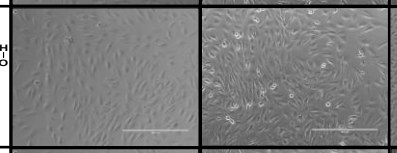	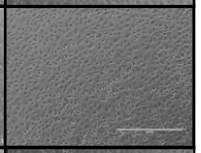	
5,6,7,8-tetramethoxy-2-(4-methoxyphenyl)-4H-chromen-4-one (**ONGC300**)	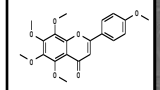	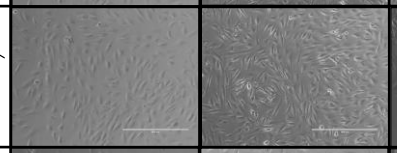	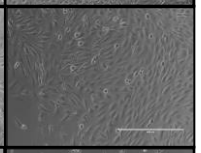	
2-(2-methoxyphenyl)-4H-chromen-4-one (**ONGD300**)	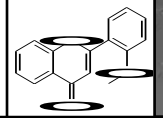	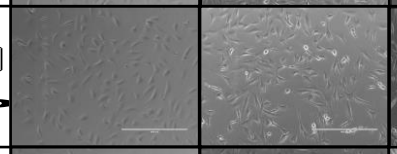	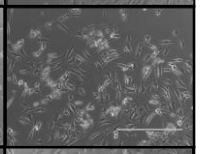	
5,7-dihydroxy-2-(2,3,4-trihydroxyphenyl)-4H-chromen-4-one (**ONGE300**)	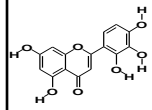	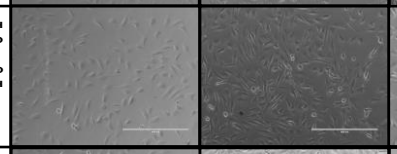	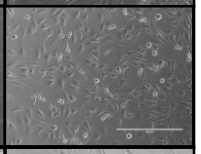	
5,7-dihydroxy-3,6-dimethoxy-2-phenyl-4H-chromen-4-one (**ONGF300**)	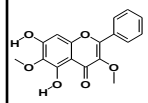	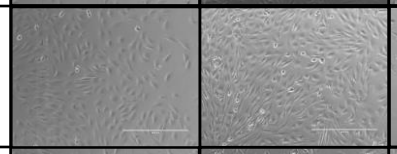	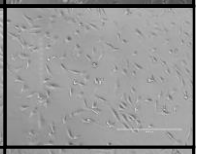	
2-(3,4-dihydroxyphenyl)-5-hydroxy-3,6,7-trimethoxy-4H-chromen-4-one (**ONGG300**)	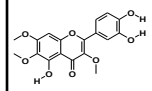	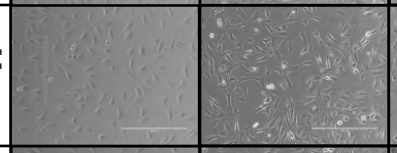	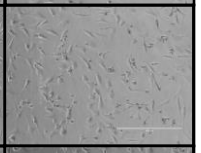	
5,7-dihydroxy-2-(4-hydroxy-3-methoxyphenyl)-3,6-dimethoxy-4H-chromen-4-one (**ONGH300**)	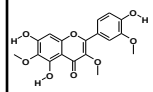	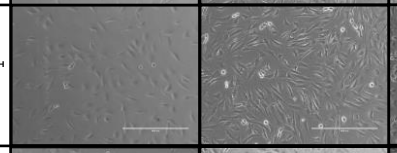	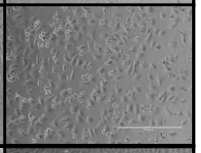	
DMEM only		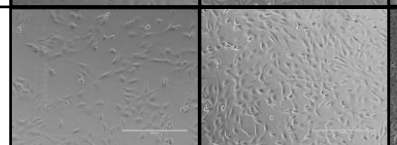	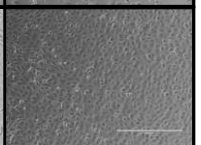	

Name	Structure	PDGF treat 전	PDGF treat 24 hr	Analogue treat 24 hr
7-hydroxy-2-phenyl-4H-chromen-4-one (**ONGA400**)	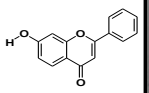	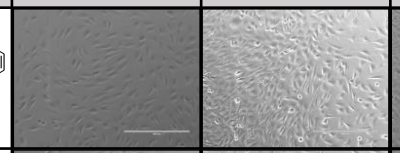	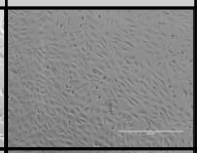	
5,7-dihydroxy-6,8-dimethoxy-2-(4-methoxyphenyl)-4H-chromen-4-one (**ONGB400**)	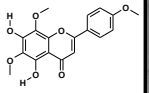	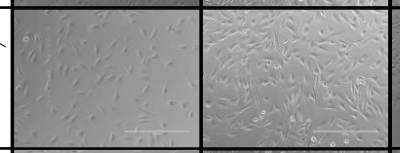	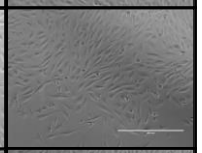	
2-(3,4-dimethoxyphenyl)-5,7,8-trimethoxy-4H-chromen-4-one (**ONGC400**)	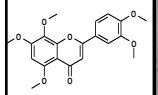	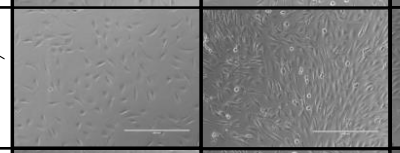	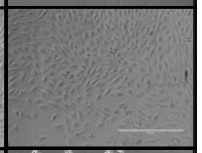	
5,7-dihydroxy-2-(3-hydroxy-4-methoxyphenyl)-3,6-dimethoxy-4H-chromen-4-one (**ONGD400**)	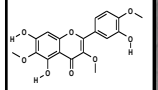	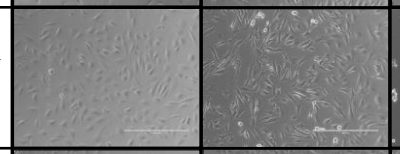	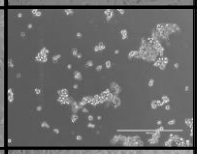	
5-hydroxy-6,7-dimethoxy-2-phenyl-4H-chromen-4-one (**ONGE400**)	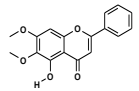	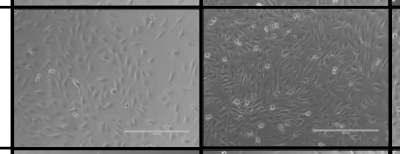	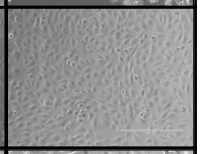	
5-hydroxy-2-phenyl-4H-chromen-4-one (**ONGF400**)	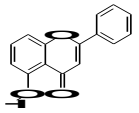	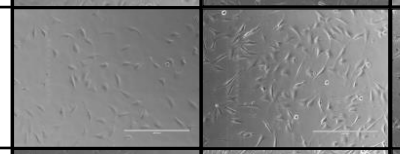	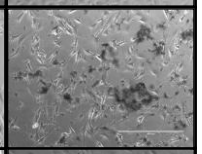	
5,6,7-trimethoxy-2-(4-methoxyphenyl)-4H-chromen-4-one **(ONGG400)**	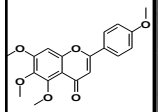	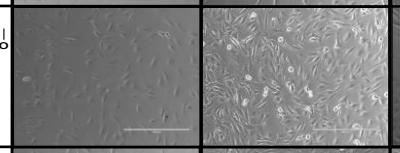	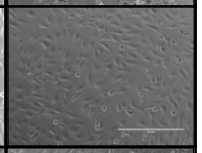	
2-(4-methoxyphenyl)-4H-chromen-4-one (**ONGH400)**	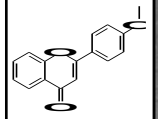	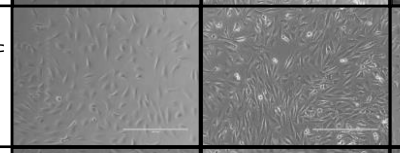	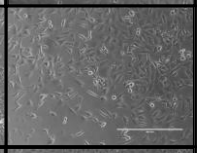	
PDGF only		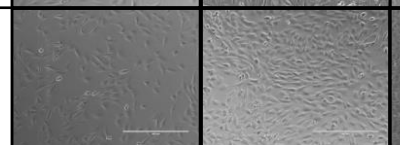		

Supplementary Figure. 10-2

TGFβ 24h

TGFβ 24h + Eupatilin 24h

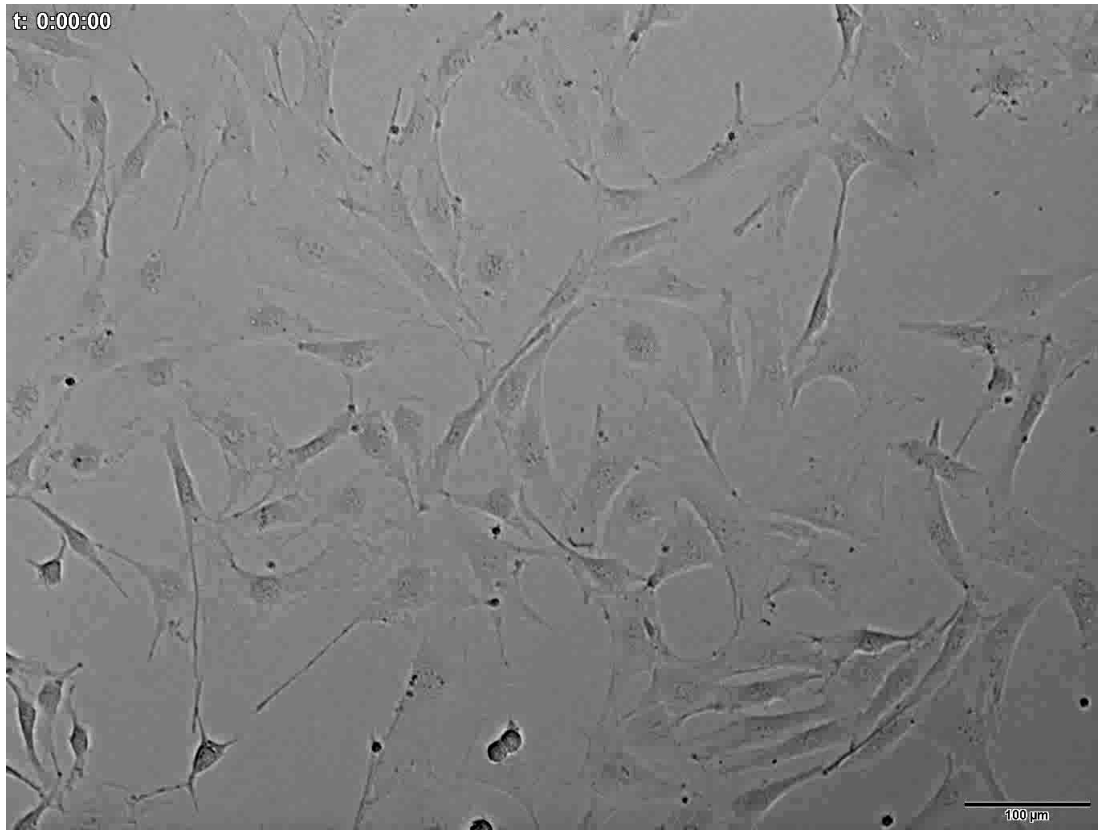

Supplementary Figure. 11

A)

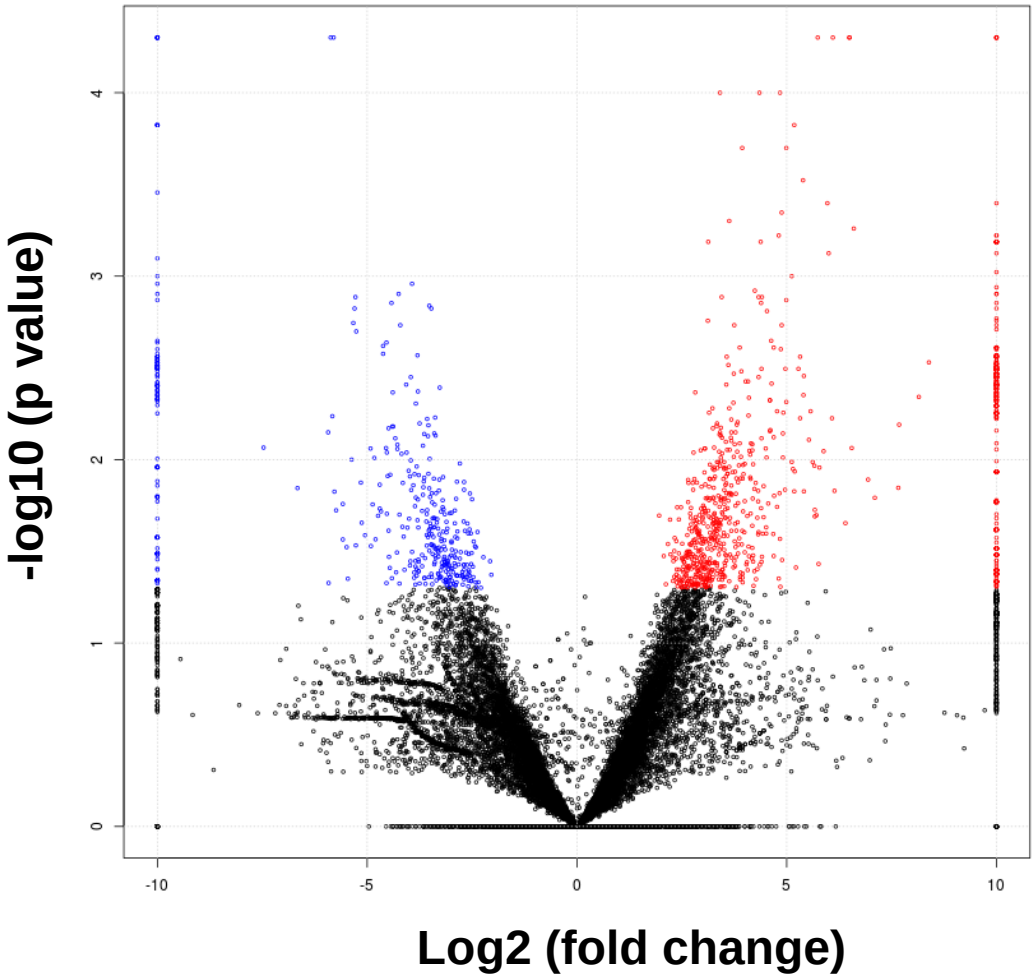

B)

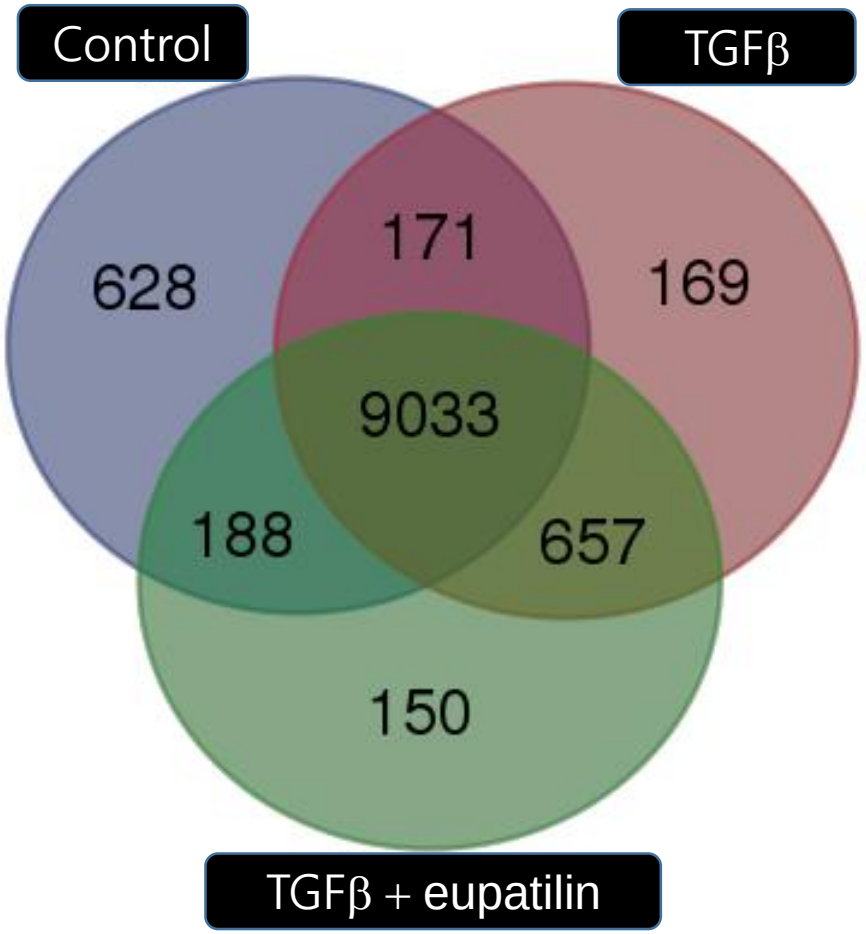

mRNA-Seq

Supplementary Figure. 12

Simultaneous stimulation

A) Sample correlation

	Non treated control	TGF-β	Euptilin
Non treated control	-	0.805	0.854
TGF-β	0.805	-	0.901
Eupatilin	0.854	0.901	-

B) GO (Gene Ontology) enrichment

No.	Name	# DEG	# GO	Molecular function	Biological function	Cellular component
1	Non treated control vs TGF-β	1886	7427	57 / 1208 (4.7 %)	228 / 5589 (4.8 %)	42 / 630 (6.7 %)
2	TGF-β vs Eupatilin	1952	7301	56 / 11161 (4.8 %)	160 / 5481 (2.9 %)	46 / 659 (7.0 %)
3	Eupatilin vs Non treated control	800	6424	22 / 987 (2.2 %)	263 / 4939 (5.3 %)	24 / 498 (4.8 %)

Supplementary Table 1

Sequential stimulation

A) Sample correlation

	Non treated control	TGF-β	Eupatilin
Non treated control	-	0.977	0.810
TGF-β	0.977	-	0.865
Eupatilin	0.810	0.854	-

B) GO (Gene Ontology) enrichment

No.	Name	# DEG	# GO	Molecular function	Biological function	Cellular component
1	Non treated control vs TGF-β	563	5628	31 / 751 (4.1 %)	436 / 4444 (9.8 %)	34 / 433 (7.9 %)
2	TGF-β vs Eupatilin	1244	5936	84 / 964 (8.7 %)	431 / 4431 (9.7 %)	111 / 541 (20.5 %)
3	Eupatilin vs Non treated control	1281	6039	79 / 962 (8.2 %)	378 / 4483 (8.4 %)	109 / 594 (18.4 %)

Supplementary Table 2

NO.	Function	Genes
I.	Cytoskeletal proteins Hub	TNNI1 & TNNI2
		Tm2
		TAGLN
		ACTA2
		MYH9 & MYH11
		LMOD1
		ACTG2
		LAMA4
II.	Collagen proteins Hub	COL4A5 & COL4A6
		COL5A1 & COL5A3
		COL6A3
		COL8A1 & COL8A5
		Col11a1
		COL12A1
		COL15A1
III.	Cell cycle proteins Hub-1	CCNB1
		Gadd45a
		CCNF
		ASPM
		Nek2
		OPTN
IV.	Cell cycle proteins Hub-2	CCND1
		CDK14
		C-Fos
		Junb
		CCL2
		CCL7

NO.	Function	Genes
V.	CD44 relation proteins Hub	Cd44
		Hyou1
		Ncam
		CALR
		Irgm1
		Parp4
		Parp9
		Pdia4 & Pdia6
VI.	Fibrillin proteins Hub	Efemp2
		Fbn5
		Fbn2
		Eln
		Fbn1
VII.	Transforming Growth Factor Beta 2 proteins Hub	Rora
		Npas2
		Serpine1
		Tgfb2
		Figf
VIII.	Semaphorin & Vldr acceptor proteins hub	PLXND1
		SEMA3E
		SEMA3A
		NRP1
		LDLR
		Ngf

Major network nods of TGFβ-Eupatilin Interactome Genes

NO.	Genes
1	Integrin β3
2	Integrin α1
3	Integrin β4
4	Protein kinase Cα
5	Lef1
6	Slug
7	Cadherin1 (=E-Cadherin)
8	Adenylate cyclase 9
9	Spp1 (= Osteopointin)
10	Fibrilin1
11	Dedicator of cytokinesis 1 (Dock1)
12	Syk2
13	Notch4

Supplementary Table 3

Eupatilin-repressible genes

NO.	Description (Abbreviation)	Log2fc	p-value
1	Actin, gamma2 (Actg2)	-5.83	0.00005
2	Periostin (Postn)	-4.92	0.00005
3	Collagen, type XI, alpha 1 (Col11a1)	-3.11	0.00005
4	Fibronectin 1 (Fn1)	- infinite	0.0002
5	Thrombospondin, type I domain containing 7A (Thsd7a)	-5.06	0.0002
6	TraB domain containing 2B (Trabd2b)	-2.75	0.0003
7	Collagen type XV, alpha 1 (Col5a1)	-2.26	0.00055
8	Slit homolog 3 (Slit3)	-3.65	0.00065
9	Cell migration inducing protein, hyaluronan biding (Cemip)	-2.75	0.00095
10	Inhibition beta-A (Inhba)	-2.19	0.0015
11	Spectrin alpha, erythrocytic 1 (Spta1)	-4.01	0.00165
12	Exocyst complex component 4 (Exoc4)	-2.9	0.0019
13	A disintegrin-like and metallopeptidase with thrombospondin type 1 motif 12 (Adamts12)	-2.09	0.0025
14	Ephrin B2 (Efnb2)	-1.92	0.0038
15	c-fos induced growth factor (Figf)	-2.49	0.0044
16	Elastin (Eln)	-3.28	0.00555
17	Heparan sulfate 6-O-sulfotransferase 2 (Hs6st2)	-3.26	0.0056
18	Perlecan (Heparan sulfate proteoglycan2) (Hspg2)	- infinite	0.0057
19	Tubulin-specific chaperone d (Tbcd)	-2.11	0.00595
20	Natriuretic peptide receptor 3 (Npr3)	-2.82	0.00675
21	Serin (or cysteine) peptidase inhibitor, clade F, member 1 (Serpinf1)	-1.99	0.00685
22	TLC domain-containing protein 2 (Tlcd2)	- infinite	0.0074
23	Fras 1 related extracellular matrix protein 1 (Frem1)	-2.36	0.0075
24	Caldesmon 1 (Cald1)	- infinite	0.0074
25	Lysyl oxidase-like 2 (Loxl2)	-1.93	0.0078
26	Tissue inhibitor of metalloproteinase 3 (Timp3)	- infinite	0.00785
27	Collagen, type III, alpha 1 (Col3a1)	- infinite	0.0083
28	Protein disulfide isomerase associated 6 (Pdia6)	-1.85	0.00835
29	Pleiotrophin (Ptn)	-2.06	0.00875
30	Prostate androgen-regulated mucin-like protein 1 (Parm1)	-1.57	0.01225
31	Dihydropyrimidinase-like 3 (Dpysl3)	- infinite	0.0138
32	Collagen, type XII, alpha 1 (Col12a1)	-2.02	0.01435
33	Crystallin, zeta (quinone reductase)-like 1 (Cryzl1)	- infinite	0.01475
34	Calumenin (Calu)	- infinite	0.015
35	Follistatin-like 1 (Fstl1)	- infinite	0.0156
36	Vinculin (Vcl)	- infinite	0.01575
37	Cyclin D2 (Ccnd2)	-2.29	0.01585
38	A disintegrin-like and metallopeptidase (reprolysin type) with thrombospondin type 1 motif 2	-2.08	0.1685
39	Dysferlin (Dysf)	-2.06	0.01765
40	Olfactomedin 2 (Olfm2)	-1.9	0.01845
41	Ubiquitin-like modifier activating enzyme 1 (Uba1)	- infinite	0.01855
42	Leprecan 1 (Lepre1)	-1.75	0.01865
43	Prosaposin (Psap)	- infinite	0.01875
44	Latent transforming growth factor beta binding protein 1 (Ltbp1)	-3.32	0.01985
45	Spectrin beta, non-erythrocytic 1 (Sptbn1)	- infinite	0.02
46	Palladin, cytoskeletal associated protein (Palld)	- infinite	0.02005
47	Protein FAM 53B (Fam53b)	- infinite	0.02015
48	Caveolin 1, Caveolae protein (Cav1)	-1.76	0.02025
49	Nischarin (Nisch)	infinite	0.02075
50	Fibronectin type III domain containing 1 (Fndc1)	-1.75	0.02105
51	Tropomyosin 1, alpha (Tpm1)	- infinite	0.02145
52	Doublecortin-like kinase 1 (Dclk1)	-1.54	0.023

NO.	Description (Abbreviation)	Log2fc	p-value
53	Actin alpha 4 (Actn4)	- infinite	0.0241
54	Colony stimulating factor 1 (macrophage) (Csf1)	-2.15	0.02535
55	Tenascin C (Tnc)	-5.1	0.02575
56	Intersectin 1 (SH3 domain protein 1A) (Itsn1)	- infinite	0.0263
57	Transforming, acidic coiled-coil containing protein 2 (Tacc2)	- infinite	0.0267
58	Pleckstrin and sec7 domain containing 3 (Psd3)	-1.43	0.0275
59	C-terminal-binding protein 2 (Ctbp2)	- infinite	0.0277
60	Heat shock protein 90, alpha (cytosolic), class A member 1(Hsp90aa1)	- infinite	0.029
61	Septin2 (Sept2)	- infinite	0.02975
62	Epidermal growth factor-containing fibulin-like extracellular matrix protein 2 (Efemp2)	-1.66	0.03005
63	EH-domain containing 2 (Ehd2)	- infinite	0.03025
64	Coatomer protein complex, subunit gamma 1 (Copg1)	- infinite	0.03045
65	v-myc myelocytomatosis viral related oncogene, neuroblastoma derived (Mycn)	-2.05	0.031
66	Lethal giant larvae homolog 1 (Llgi1)	- infinite	0.0331
67	Interleukin 18 receptor accessory protein (Il18rap)	-1.69	0.0332
68	Willians-Beuren syndrome chromosome reion 17 homolog (Wbscr17)	-2.83	0.03325
69	Collagen type 1 alpha 1 (Col1a1)	-1.64	0.0334
70	Synaptopodin (Synpo)	- infinite	0.03375
71	Integrin beta 5 (Itgb5)	- infinite	0.0342
72	Tankyrase, TRF1-interacting ankyrin-related ADP-rebose polymerase 2 (Tnks2)	- infinite	0.0349
73	Procollagen-lysine, 2-oxoglutarate 5-dioxygenase 3 (Plod3)	-2.01	0.0355
74	BTAF1 RNA polymerase II, B-TFIID transcription factor-associated (Btaf1)	- infinite	0.0356
75	Dynein cytoplasmic 1 heavy chain 1 (Dync1h1)	- infinite	0.03565
76	Aurora kinase A (Aurka)	-15.3	0.03595
77	WNK lysine deficient protein kinase 1 (Wnk1)	- infinite	0.03685
78	Collagen type VII alpha1 (Col7a1)	-15.2	0.03715
79	Procollagen-proline, 2-oxoglutarate 4-dioxygenase (proline 4-hydroxylase), alpha 1 polypeptide (P4ha1)	-1.81	0.0375
80	Spectrin repeat containing nuclear envelope 2 (Syne2)	- infinite	0.0376
81	Cell cycle associated protein 1 (Caprin1)	- infinite	0.0382
82	Calreticlin (Calr)	-1.74	0.03845
83	Endoglin (Eng)	- infinite	0.03895
84	Microtubule-associated protein 4 (Map4)	- infinite	0.039
85	rho/rac guanine nucleotide exchange factor (GEF) 2 (Arhgef2)	- infinite	0.03915
86	Inositol hexakisphosphate kinase 1 (Ip6k1)	- infinite	0.03985
87	TEA Domain Transcription factor 1 (TEAD1)	- infinite	0.04005
88	Procollagen lysine, 2-oxoglutarate 5-dioxygenase 2 (Plod2)	-1.48	0.0402
89	Family with sequence similarity 175, member B (Fam175b)	- infinite	0.0413
90	ArfGAP with SH3 domain, ankyrin repeat and PH domain 1 (Asap1)	- infinite	0.0414
91	Laminin, alpha 4 (Lama4)	-1.29	0.04145
92	Serine (or cysteine) peptidase inhibitor, clade E, member 1 (Serpine 1)	-1.78	0.0419
93	Importin-4 (Ipo4)	- infinite	0.04235
94	Transformation/ transcription domain-associated protein (Trrap)	- infinite	0.043
95	Surfeit 1 (SURF1)	- infinite	0.044
96	Oxysterol binding protein-like 9 (Osbpl9)	- infinite	0.0458
97	Endoplasmic reticulum-golgi intermediate compartment 1 (ERGIC1)	-1.26	0.0465
98	Ring finger protein 145 (Rnf145)	- infinite	0.04665
99	AXL receptor tyrosine kinase (Axl)	- infinite	0.048
100	Latent transforming growth factor beta binding protein 2 (Ltbp2)	- infinite	0.04845
101	Latent transforming growth factor beta binding protein 4 (Ltbp4)	- infinite	0.0492
102	Multiple coagulation factor deficiency 2 (Mcfd2)	-1.28	0.04935
103	Thymoma viral proto-oncogene 1 (Akt1)	- infinite	0.04985

Supplementary Table 4

Test group	Bleomycin administration	Eupatilin administration
Normal control group	-	-
Bleomycin-administered group	40 μg/head	vehicle
Bleomycin + 1 μg of eupatilin-administered group	40 μg/head	1 μg/20 μL
Bleomycin + 5 μg of eupatilin-administered group	40 μg/head	5 μg/20 μL
Bleomycin + 10 μg of eupatilin-administered group	40 μg/head	10 μg/20 μL
Bleomycin + 20 μg of eupatilin-administered group	40 μg/head	20 μg/20 μL
Bleomycin + 40 μg of eupatilin-administered group	40 μg/head	40 μg/20 μL

Supplementary Table 5